Role of D1-His190 in Proton-Coupled Electron Transfer Reactions in Photosystem II: A Chemical Complementation Study†

Anna-Maria A. Hays,‡ Ilya R. Vassiliev,§ John H. Golbeck,§ and Richard J. Debus*,‡

Department of Biochemistry, University of California at Riverside, Riverside, California 92521-0129, and Department of Biochemistry and Molecular Biology, The Pennsylvania State University, University Park, Pennsylvania 16802

Received March 4, 1998; Revised Manuscript Received June 3, 1998

ABSTRACT: Recent models for water oxidation in photosystem II propose that His190 of the D1 polypeptide facilitates electron transfer from tyrosine Y_Z to P_{680}^+ by accepting the hydroxyl proton from Y_Z. To test these models, and to further define the role of D1-His190 in the proton-coupled electron transfer reactions of PSII, the rates of P_{680}^+ reduction, Y_Z oxidation, Q_A^- oxidation, and $Y_Z^\bullet$ reduction were measured in PSII particles isolated from several D1-His190 mutants constructed in the cyanobacterium *Synechocystis* sp. PCC 6803. These measurements were conducted in the absence and presence of imidazole and other small organic bases. In all mutants examined, the rates of P_{680}^+ reduction, Y_Z oxidation, and $Y_Z^\bullet$ reduction after a single flash were slowed dramatically and the rate of Q_A^- oxidation was accelerated to values consistent with the reduction of P_{680}^+ by Q_A^- rather than by Y_Z. There appeared to be little correlation between these rates and the nature of the residue substituted for D1-His190. However, in nearly all mutants examined, the rates of P_{680}^+ reduction, Y_Z oxidation, and $Y_Z^\bullet$ reduction were accelerated dramatically in the presence of imidazole and other small organic bases (e.g., methyl-substituted imidazoles, histidine, methylamine, ethanolamine, and TRIS). In addition, the rate of Q_A^- oxidation was decelerated substantially. For example, in the presence of 100 mM imidazole, the rate of electron transfer from Y_Z to P_{680}^+ in most D1-His190 mutants increased 26−87-fold. Furthermore, in the presence of 5 mM imidazole, the rate of $Y_Z^\bullet$ reduction in the D1-His190 mutants increased to values comparable to that of Mn-depleted wild-type PSII particles in the absence of imidazole. On the basis of these results, we conclude that D1-His190 is the immediate proton acceptor for Y_Z and that the hydroxyl proton of Y_Z remains bound to D1-His190 during the lifetime of $Y_Z^\bullet$, thereby facilitating the reduction of $Y_Z^\bullet$.

Photosynthetic water oxidation takes place in photosystem II (PSII)[1] near the lumenal surface of the thylakoid membrane. PSII is a multisubunit, integral membrane protein complex that utilizes light energy to oxidize water and reduce plastoquinone (for review, see refs *1*−*7*). The oxygen-evolving catalytic site contains four Mn ions that are arranged in a multinuclear cluster. The Mn cluster accumulates oxidizing equivalents in response to photochemical events within PSII and then catalyzes the oxidation of two water molecules, releasing one molecule of O_2 as a byproduct. The photochemical events that precede water oxidation take place in a heterodimer of two homologous polypeptides known as D1 and D2. These events are initiated by the capture of light by an antenna complex that is located peripherally with respect to PSII. The excitation energy is transferred to the photochemically active chlorophyll species known as P_{680}. Excitation of P_{680} results in formation of the charge-separated state, $P_{680}^+Q_A^-$, where Q_A is a molecule of plastoquinone. The P_{680}^+ radical rapidly oxidizes tyrosine Y_Z (Tyr161 of the D1 polypeptide), forming the neutral radical, $Y_Z^\bullet$. This radical in turn oxidizes the Mn cluster, while Q_A^- reduces the secondary plastoquinone, Q_B. Subsequent charge separations result in further oxidation of the Mn cluster. During each catalytic cycle, the Mn cluster cycles through five oxidation states termed S_n, where n denotes the number of oxidizing equivalents stored. The S_1 state predominates in dark-adapted samples. The S_3 state may have one oxidizing equivalent localized on a Mn ligand. The S_4 state is a transient intermediate that reverts to the S_0 state with the concomitant release of O_2. In addition to Y_Z, PSII contains a second redox-active tyrosine residue, known as Y_D (Tyr160 of the D2 polypeptide in the numbering system of *Synechocystis* sp. PCC 6803). This tyrosine residue is also oxidized by P_{680}^+, but its function remains unknown. Y_Z

† This work was funded by the National Institutes of Health (Grant GM 43496 to R.J.D.) and by the National Science Foundation (Grant MCB 972366 to J.H.G.).

* To whom correspondence should be addressed. Phone: (909) 787-3483. Fax: (909) 787-4434. E-mail: debusrj@citrus.ucr.edu.

‡ University of California at Riverside.

§ The Pennsylvania State University.

[1] Abbreviations: Chl, chlorophyll *a*; DCBQ, 2,6-dichloro-*p*-benzoquinone; DCMU, 3-(3,4-dichlorophenyl)-1,1-dimethylurea; ENDOR, electron nuclear double-resonance; fwhm, full width at half-maximum; *k*, rate constant (inverse of the time required for amplitude to reach 1/e of its initial value); PSII, photosystem II; P_{680}, chlorophyll species that serves as the light-induced electron donor in PSII; Y_Z, tyrosine residue that mediates electron transfer between the Mn cluster and P_{680}^+; Y_D, tyrosine residue known to act as an alternate electron donor to P_{680}^+; Q_A, primary plastoquinone electron acceptor; Q_B, secondary plastoquinone electron acceptor; MES, 2-(*N*-morpholino)ethanesulfonic acid; TES, 2-{[tris(hydroxymethyl)methyl]amino}ethanesulfonic acid; CHES, 2-(*N*-cyclohexylamino)ethanesulfonic acid; TRIS, tris(hydroxymethyl)aminomethane; wild-type*, strain of *Synechocystis* sp. PCC 6803 constructed in the same fashion as the mutants, but containing the wild-type *psb*A-2 gene.

S0006-2960(98)00510-8 CCC: $15.00
Published on Web 07/18/1998

and Y_D appear to be located symmetrically with respect to the probable C_2 symmetry axis of the PSII reaction center (*8*).

The possible role of Y_Z in the mechanism of water oxidation is currently being intensely debated. Two recent models postulate that Y_Z participates directly in water oxidation by abstracting protons (*2*, *9*−*11*) or hydrogen atoms (*12*−*20*) from water-derived ligands of the Mn cluster. In these models, protons are transported vectorially from the Mn cluster and toward the lumen by Y_Z. The models were developed in response to data showing that Y_Z is located very close to the Mn cluster (*9*−*11*) [recent simulations yield Mn−Y_Z distances of 7.5−11.5 Å (*21*−*23*)], that $Y_Z^•$ is rotationally mobile in both Mn-depleted (*12*, *13*) and Ca^{2+}-depleted (*9*) PSII preparations, and that the hydrogen bonding of $Y_Z^•$ is disordered in Mn-depleted preparations (*11*, *24*−*27*). Consistent with these models, $Y_Z^•$ appears to accept multiple hydrogen bonds in acetate-treated (*11*, *22*) and Ca^{2+}-depleted (*19*) PSII preparations, whereas $Y_D^•$ accepts only one (*11*, *28*). In addition, recent data suggest that the Mn cluster is structurally coupled to a tyrosine residue, possibly Y_Z (*29*). The competing models propose either that $Y_Z^•$ serves only to transfer electrons from the Mn cluster to P_{680}^+ (*30*−*32*) [as proposed earlier (*33*, *34*)] or that, additionally, the hydroxyl proton released from Y_Z remains near $Y_Z^•$ and increases the oxidizing power of the Mn cluster via an electrostatic interaction (*32*). These models are based on pH-dependent measurements of proton release (*31*, *32*, *35*−*41*) and pH-dependent measurements of chlorophyll absorbance band shifts (*25*, *32*, *36*, *38*−*43*). The latter have been interpreted as reflecting electrochromism that is caused by a positive charge retained near $Y_Z^•$ and the Mn cluster during part of the S-state cycle. This interpretation conflicts with the proton and hydrogen atom abstraction models; these models predict that the vectorial transfer of protons from the Mn cluster to the lumen would prevent the retention of charge on the Mn cluster or its environment.

In all of the models described above, the reduction of P_{680}^+ is facilitated by the deprotonation of Y_Z by a nearby base. This base is presumed to be His190 of the D1 polypeptide (*2*, *3*, *13*−*16*, *18*, *44*). This presumption is based on modeling studies that place Y_Z and His190 close together (*44*−*46*), on data showing that D2-His189 (in the numbering system of *Synechocystis* sp. PCC 6803) is the proton acceptor for Y_D (*28*) (also see refs *27* and *47*−*49*), and on mutagenesis studies showing that electron transfer from Y_Z to P_{680}^+ is impaired in D1-His190 mutants (*50*−*54*).

To further define the role of D1-His190 in Y_Z function, we have replaced D1-His190 with the following residues: Lys, Arg, Asp, Glu, Asn, Gln, Ser, Thr, Cys, Tyr, Phe, Leu, Val, Ala, and Gly. All mutants were constructed in the cyanobacterium *Synechocystis* sp. PCC 6803. All of the mutants were obligate photoheterotrophs, and only the Lys and Arg mutants evolved O_2 at significant rates (10−13% compared to that of wild-type* cells (*54*; unpublished results). On the basis of chlorophyll *a* fluorescence measurements conducted in vivo (*55*), electron transfer from Y_Z to P_{680}^+ was determined (indirectly) to be severely disrupted in all 15 of these mutants (*54*; unpublished results). In this study, we have directly measured the rates of Y_Z oxidation, P_{680}^+ reduction, Q_A^- oxidation, and $Y_Z^•$ reduction in PSII particles isolated from seven D1-His190 mutants. These measurements were conducted in the presence and absence of imidazole and other small organic bases. The strategy of replacing amino acid side chains with exogenous molecules (i.e., "chemical rescue") is well-established (*56*−*65*) and has been widely employed to probe the function of specific histidine residues as acid−base catalysts (*66*, *67*) or as ligands to metal ions (*68*−*72*). In all seven mutants, the rates of P_{680}^+ reduction, Y_Z oxidation, and $Y_Z^•$ reduction after a single flash were slowed dramatically and the rate of Q_A^- oxidation was accelerated to values consistent with the reduction of P_{680}^+ by Q_A^- rather than by Y_Z. There appeared to be little correlation between these rates and the nature of the residue substituted for D1-His190. However, in six mutants, the rates of P_{680}^+ reduction, Y_Z oxidation, and $Y_Z^•$ reduction were accelerated dramatically in the presence of imidazole and other small organic bases (e.g., methyl-substituted imidazoles, histidine, methylamine, ethanolamine, and TRIS). In addition, the rate of Q_A^- oxidation was slowed substantially. We conclude that D1-His190 is the immediate proton acceptor for Y_Z and that the hydroxyl proton of Y_Z remains bound to D1-His190 during the lifetime of $Y_Z^•$.

MATERIALS AND METHODS

Construction of Site-Directed Mutants. All mutants were constructed in the *psb*A-2 gene of the unicellular cyanobacterium *Synechocystis* sp. PCC 6803. All His190 mutants except H190S were constructed as described previously (*54*, *55*). The wild-type* strain, described previously (*54*, *55*), was constructed in an identical manner, but with a transforming plasmid that carried no site-directed mutation. The designation wild-type* differentiates this strain from the native wild-type strain that contains all three *psb*A genes and is sensitive to antibiotics. The mutants H190S and Y161F were constructed in a strain of *Synechocystis* that lacks PSI and *apc*E function (*73*).

Propagation of Cultures. Cells were maintained on solid BG-11 media (*74*) containing 5 mM glucose and 10 μM DCMU as described previously (*55*), except that the concentration of glucose was increased to 15 mM for mutants lacking PSI and *apc*E function (*75*). The DCMU was omitted from liquid cultures. For isolation of PSII particles, cells were grown in modified 250 mL Erlenmeyer flasks (*55*) until they reached an optical density of 0.6−1.1 at 730 nm (measured with a modified CARY-14 spectrophotometer). Cells (60−120 mL per carboy) were then transferred to two 15 L carboys and grown until their optical density again reached 0.7−1.1 (typically 4−5 days for cells containing PSI and 6−7 days for cells lacking PSI). Carboys were grown at 30 °C under constant illumination and were aerated by bubbling with sterile filtered air. Constant illumination was provided by fluorescent cool-white bulbs at an intensity of 50−60 μE m^{-2} s^{-1} [measured with a LI-COR (Lincoln, NE) model LI-190 light meter].

Isolation of PSII Complexes. Thylakoid membranes and PSII particles were isolated essentially as described by Tang and Diner (*76*) with the following modifications: All buffers contained 25% (v/v) ultrapure glycerol (Gibco-BRL, Gathersville, MD), the *n*-dodecyl β-D-maltoside (ANAGRADE) was purchased from Anatrace (Maumee, OH), and the purified PSII particles were found to elute from the 350 mL DEAE-Toyopearl 650s column with purification buffer [25%

(v/v) glycerol, 50 mM MES-NaOH (pH 6.0), 20 mM $CaCl_2$, 5 mM $MgCl_2$, and 0.03% dodecyl maltoside] containing 15−20 mM $MgSO_4$. For the strains lacking PSI, thylakoid membranes were extracted with *n*-dodecyl β-D-maltoside at a concentration of 0.05−0.10 mg of Chl/mL and the extract was applied to a 40 mL DEAE-Toyopearl 650s column. This column was washed with purification buffer containing 5 mM $MgSO_4$ until most of the orange-pigmented contaminants (presumably carotenoid-binding proteins) had eluted, and then PSII was eluted with purification buffer containing 50 mM $MgSO_4$. Purified PSII particles were concentrated to 0.4−0.7 mg of Chl/mL by ultrafiltration (*76*), frozen in liquid nitrogen, and stored at −80 °C. The purified PSII particles lack Q_B (*76*).

Extraction of Mn. Wild-type* PSII particles were depleted of Mn by a procedure modified from ref *77*. Intact, O_2-evolving PSII particles were incubated at 0.2−0.3 mg of Chl/mL for 30 min at 4 °C in darkness in the presence of 5 mM NH_2OH and 1 mM EDTA. The material was then adsorbed to a Pharmacia HR 5/5 Mono-Q ion-exchange column and washed extensively (15−20 column volumes) with purification buffer to remove the NH_2OH and free Mn. The column was then inverted (*78*) and eluted slowly with purification buffer containing 0.5 M NaCl. The NH_2OH-treated PSII particles were then desalted with a Pharmacia HR 10/10 Fast Desalting Column. The residual O_2 evolution activity of the extracted preparations was 4−6% compared to that of untreated wild-type* PSII particles. The mutant PSII particles appeared to lack functional Mn ions and were not extracted to remove Mn.

Measurements of Chlorophyll Concentrations, Oxygen Evolution Rates, and Chlorophyll/Q_A Ratios. Chlorophyll *a* concentrations were determined by extraction into methanol (100-fold dilution) as described previously (*55*). An extinction coefficient of 79.24 mM^{-1} cm^{-1} at 665.2 nm was employed (*79*). Rates of light-saturated oxygen evolution were measured at 25.0 °C as described previously (*55*) except that the assay buffer contained 1 M sucrose, 50 mM MES-NaOH (pH 6.5), 25 mM $CaCl_2$, and 10 mM NaCl. Each sample contained 3−5 μg of Chl/mL, 0.4 mM 2,6-dichloro-*p*-benzoquinone (purified by sublimation), and 1 mM potassium ferricyanide. Illumination was provided by two Dolan-Jenner (Woburn, MA) model 180 fiber optics illuminators equipped with EJV bulbs. The light was passed through Dolan-Jenner infrared and red cutoff filters and directed to both sides of the sample with Dolan-Jenner fiber optic light guides. The Clark-type electrode was calibrated with hydrogen peroxide [freshly opened J. T. Baker ULTREX grade (Phillipsburg, NJ)] and catalase (*80*). The chlorophyll per Q_A ratio in PSII complexes was determined from the absorbance increase at 325 nm caused by a series of 20−40 saturating flashes administered at 50 ms intervals in the presence of hydroxylamine (*76*). Measurements were performed essentially as described previously (*81*). An extinction coefficient of 13 mM^{-1} cm^{-1} for $Q_A^- \rightarrow Q_A$ at 325 nm was employed (*82*). Samples contained 35 μg of Chl/mL, 20 mM MES-NaOH (pH 6.0), 0.04% dodecyl maltoside, 10 μM potassium ferricyanide, 40 μM DCMU, and 2 mM hydroxylamine. All preparations employed in this study contained 39−58 Chl/Q_A with the exception of H190E PSII particles, which contained 86 Chl/Q_A, and the preparation of H190R particles used in the experiments of Figure 1, which contained 74 Chl/Q_A. Ratios in excess of 39 Chl/Q_A were attributed to residual contamination by PSI (*76*).

Optical Measurements in the UV and Visible Spectra. Transient absorbance changes of Y_Z at 242 nm (ΔA_{242}), Q_A at 325 nm (ΔA_{325}), and P_{680} at 432.5 nm ($\Delta A_{432.5}$) were measured with a modified CARY-14 spectrophotometer (On-Line Instrument Systems, Inc., Bogart, GA) operated in single-beam mode (chopper motor off) with the detector housing replaced by an end-on Hamamatsu R374 photomultiplier tube and a separate amplifier (EG&G Princeton Applied Research, model 5113). The amplified output was recorded with a LeCroy 9310M digital oscilloscope. The data were stored and converted to units of absorbance on a personal computer with software developed in the Physics Department at the University of California, San Diego. For measurements at 242 nm, the monitoring illumination was provided by a Hamamatsu L-1403 deuterium lamp. For measurements at 325 and 432.5 nm, the monitoring illumination was provided by a remotely focused OSRAM HLX 64640 lamp. For measurements at 242 and 325 nm, the photomultiplier tube was protected by two Corion solar blind filters. For measurements at 432.5 nm, the photomultiplier was protected by a Corion LS-450 cutoff filter and a Melles-Griot 435.8 nm interference filter. Actinic flashes (approximately 4 μs fwhm) were provided by a Xenon Corp. (Woburn, MA) model 457A xenon flash-lamp system (0.5 μF capacitor charged to 7−8 kV). The flashes were passed through two 2 mm thick Schott WG-360 filters, two 2 mm thick Schott RG-610 filters, and one Corion LS-750 filter and were directed to the sample cuvette with a 3.8 m long flexible light guide (Schott Fiber Optics, Southbridge, MA). The cuvette containing the sample was held in a thermostated jacket. Samples were incubated in darkness for 2 min in the presence of 10 μM potassium ferricyanide to ensure oxidation of Q_A, allow equilibration with exogenous bases, and oxidize P_{700} in residual PSI. This procedure oxidized >95% of the residual P_{700}, as determined by measurements conducted at 832 nm with purified PSI particles (data not shown). For the experiments of Figure 6, samples were given 10 preflashes at 0.1 Hz to preoxidize Y_D. Kinetics were analyzed with Jandel Scientific's (San Rafael, CA) PeakFit program, version 4.0.

Optical Measurements in the Near-IR Spectrum. Transient absorbance changes of P_{680} at 810 nm (ΔA_{810}) were measured using a laboratory-built double-beam spectrophotometer described previously (*83*), with the exception that the measuring beam at 810 nm (80 mW) was provided by a TI-SPB titanium−sapphire laser (Schwartz Electro-Optics, Orlando, FL) pumped with a model 2020-05 argon ion laser (Spectra-Physics, Mountain View, CA) emitting all lines at 5 W output power. The flash excitation was provided by a frequency-doubled, Q-switched DCR-11 Nd:YAG laser (Spectra-Physics) operating at 532 nm with a pulse fwhm of 10 ns at a flash energy of 22 mJ. Samples were treated and data were analyzed as described in the previous paragraph.

RESULTS

Scheme 1 depicts the electron transfer reactions that take place in PSII particles that lack the Mn cluster and Q_B (*84*, *85*). After an actinic flash, at least three species compete

Scheme 1

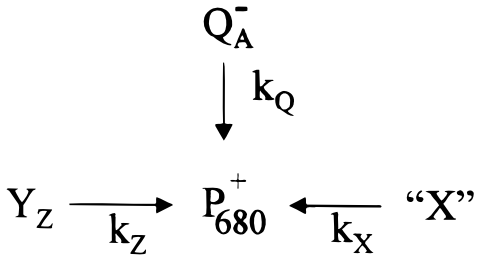

for the reduction of P_{680}^+: Y_Z (with rate constant k_Z), Q_A^- (with rate constant k_Q), and other, unidentified electron donors (collectively denoted X, with rate constant k_X). Because the actinic flashes in our experiments were applied at 0.1 Hz, $Y_D^\bullet$ should remain oxidized during data collection; therefore, X should not include Y_D. Reduced-minus-oxidized difference spectra (obtained as described in ref *81*) showed that less than 2% of the cytochrome b_{559} in His190 mutant PSII particles was in the reduced form (not shown); therefore, X should not include cytochrome b_{559}. The observed rate of P_{680}^+ reduction is the sum of the intrinsic rate constants, $k_Z + k_Q + k_X$. The individual rate constants can be estimated by monitoring P_{680}^+ reduction [at 432.5 (*86*−*88*) or 810 nm (*89*, *90*)], Q_A^- oxidation [at 325 nm (*82*, *87*, *88*, *91*, *92*)], and Y_Z oxidation [near 242 nm (*87*, *88*, *91*−*94*)] under the same experimental conditions. Because k_Z, k_Q, and k_X represent parallel reactions, the rapid kinetic phase observed at each wavelength after an actinic flash corresponds to the sum of these three intrinsic rate constants. The fraction of Q_A^- recombining with P_{680}^+ (measured at 325 nm) provides the ratio $k_Q/(k_Z + k_Q + k_X)$. The fraction of $Y_Z^\bullet$ formed after a flash (measured at 242 nm) provides the ratio $k_Z/(k_Z + k_Q + k_X)$. Impaired oxidation of Y_Z by P_{680}^+ should be manifested as slowed reduction of P_{680}^+, an increase in the fraction of Q_A^- that recombines with P_{680}^+, and a decrease in the fraction of $Y_Z^\bullet$ formed after a flash.

P_{680}^+ Reduction Measured at 432.5 nm. The flash-induced formation and reduction of P_{680}^+, as monitored at 432.5 nm, is shown in Figure 1. At this wavelength, Q_A^- (*82*, *87*, *88*, *91*, *92*) and $Y_Z^\bullet$ (*87*, *88*, *91*−*94*) make only minor contributions to the absorbance changes. Studies at 810 nm (see below) showed that an incubation time of 2 min at room temperature under the assay conditions described in the legend to Figure 1 was sufficient to equilibrate samples with imidazole. Incubation times longer than 30 min at room temperature accelerated P_{680}^+ reduction in His190 mutant PSII particles even in the absence of imidazole, suggesting deterioration of sample. Therefore, signal averaging was completed within 15−30 min of sample dilution.

In all of the His190 mutants (e.g., Figure 1C−F), the reduction of P_{680}^+ was dramatically slower than that in the Mn-depleted wild type* [the kinetics in the wild-type* PSII particles (Figure 1A) were too rapid to be resolved on this time scale]. Indeed, the rates of P_{680}^+ reduction in the His190 mutants resemble (but are somewhat slower than) the rate in PSII particles that lack Y_Z [Y161F PSII particles, Figure 1B (*88*)]. There appears to be no correlation between the rate of P_{680}^+ reduction and the nature of the residue substituted for His190. However, in all of the His190 mutants except H190E (Figure 1F), the reduction of P_{680}^+ was accelerated dramatically in the presence of 5−100 mM imidazole (e.g., Figure 1C−E). Imidazole also increased P_{680}^+ reduction in H190E particles (Figure 1F), but the effect was much smaller. Note that 400 mM imidazole slightly accelerated P_{680}^+ reduction in Y161F PSII particles, particles that lack Y_Z (Figure 1B, see the next section).

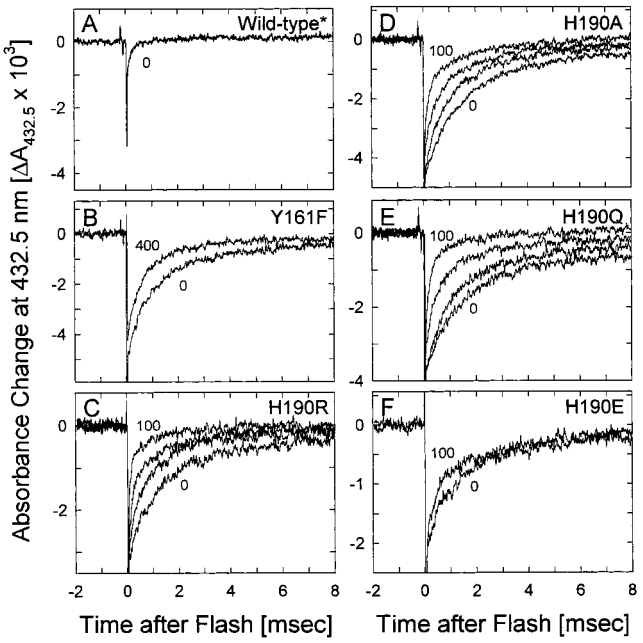

FIGURE 1: Formation and decay of P_{680}^+ in isolated PSII particles in the presence and absence of imidazole, as monitored at 432.5 nm: (A) Mn-depleted wild type* in the presence of 0 mM imidazole, (B) Y161F in the presence of 0 and 400 mM imidazole, (C) H190R in the presence of 0, 5, 20, and 100 mM imidazole, (D) H190A in the presence of 0, 5, 20, and 100 mM imidazole, (E) H190Q in the presence of 0, 5, 20, and 100 mM imidazole, and (F) H190E in the presence of 0 and 100 mM imidazole. In panels C−F, individual traces were normalized to the initial amplitude of the trace containing 0 mM imidazole. Conditions were as follows: 4.5 μg of Chl in 0.5 mL of 20 mM TES, 0.04% *n*-dodecyl β-D-maltoside, 10 μM $K_3Fe(CN)_6$, pH 7.5, and 21 °C. Samples were incubated in darkness for 2 min before the monitoring beam was turned on. Red-filtered xenon flashes (4 μs fwhm) were applied at 10 s intervals. Each trace represents the average of 100 sweeps.

P_{680}^+ Reduction Measured at 810 nm. The flash-induced formation and reduction of P_{680}^+, as monitored at 810 nm, is shown in Figure 2 (note the logarithmic time scale). These data permit a direct comparison of Mn-depleted wild-type*, Y161F, and His190 mutant PSII particles. As observed in Figure 1, the rates of P_{680}^+ reduction were dramatically slower in Y161F, H190A, and H190Q (Figure 2B−D) than in Mn-depleted wild-type* particles (Figure 2A). The overall half-decay times of P_{680}^+ reduction were approximately 2 μs, 530 μs, 1.05 ms, and 1.3 ms, respectively, for the Mn-depleted wild-type*, Y161F, H190A, and H190Q PSII particles, respectively. The overall half-decay time of P_{680}^+ reduction in the wild-type* particles (Figure 2A) was similar to that observed in inactivated particles from pea at this pH value (*32*). The overall kinetics resembled earlier data for NH_2OH- or TRIS-treated PSII preparations (*95*−*99*). The data of Figure 2 show that P_{680}^+ reduction is slowed approximately 270-, 530-, and 650-fold in the Y161F, H190A, and H190Q PSII particles, respectively, at pH 7.5. At pH 9.5, mutants H190R, H190Q, H190G, and H190K had overall half-decay times of 100−400 μs (e.g., see below, Figure 5F), whereas Mn-depleted wild-type* PSII particles

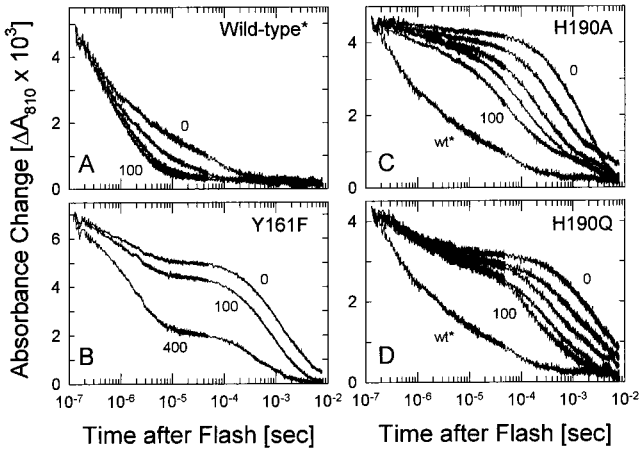

FIGURE 2: Formation and decay of P_{680}^+ in isolated PSII particles in the presence and absence of imidazole, as monitored at 810 nm (note the logarithmic time scale): (A) Mn-depleted wild type* in the presence of 0, 10, 50, and 100 mM imidazole, (B) Y161F in the presence of 0, 100, and 400 mM imidazole, (C) H190A in the presence of 0, 10, 30, 50, and 100 mM imidazole, and (D) H190Q in the presence of 0, 10, 30, 50, and 100 mM imidazole. In each panel, the individual traces were normalized to the initial amplitude of the trace containing 0 mM imidazole. In panels C and D, the normalized trace of the wild type* in the presence of 0 mM imidazole (wt*) is reproduced from panel A for comparison. Conditions were as follows: 10 μg of Chl in 0.35 mL of 20 mM TES, 0.04% *n*-dodecyl β-D-maltoside, 10 μM $K_3Fe(CN)_6$, pH 7.5, and 21 °C. Samples were incubated in darkness for 2 min before being placed in the probe beam. Laser flashes (532 nm, 10 nm fwhm) were applied at 10 s intervals. Each trace represents the average of 10−16 sweeps.

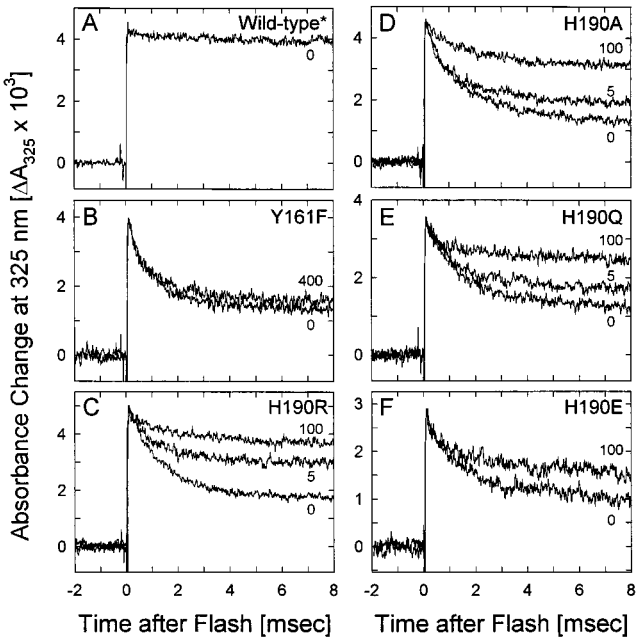

FIGURE 3: Formation and decay of Q_A^- is isolated PSII particles in the presence of 0, 5, 100, and 400 mM imidazole, as monitored at 325 nm: (A) Mn-depleted wild type*, (B) Y161F, (C) H190R, (D) H190A, (E) H190Q, and (F) H190E. In panels C−F, individual traces were normalized to the initial amplitude of the trace containing 0 mM imidazole. Conditions were as follows: 8.9 μg of Chl in 0.5 mL of 20 mM TES, 0.04% *n*-dodecyl β-D-maltoside, 10 μM $K_3Fe(CN)_6$, pH 7.5, and 21 °C. Samples were incubated in darkness for 2 min before the monitoring beam was turned on. Red-filtered xenon flashes (4 μs fwhm) were applied at 10 s intervals. Each trace represents the average of 100 sweeps.

had an overall half-decay time of approximately 0.4 μs (not shown).

As observed at 432.5 nm, the rates of P_{680}^+ reduction in H190A and H190Q PSII particles measured at 810 nm were accelerated dramatically in the presence of 10−100 mM imidazole (Figure 2C,D). In the presence of 100 mM imidazole, the overall half-decay times for P_{680}^+ reduction in H190A and H190Q PSII particles decreased to approximately 47 and 90 μs, respectively. High concentrations of imidazole (100−400 mM) also accelerated P_{680}^+ reduction in Y161F PSII particles (Figure 2B). This effect is not understood, but was observed even with ultrapure imidazole. Therefore, it does not appear to be caused by a trace contaminant in the imidazole. No acceleration was caused by the addition of 50 mM KCl. Therefore, the effect is not caused by an increase in ionic strength associated with adding the imidazole. Because of this effect, we confined our analyses of His190 mutants to imidazole concentrations of ≤100 mM. At these concentrations, the effects of imidazole on His190 PSII particles were substantially larger than those on Y161F PSII particles (compare panels C and D of Figure 2 with panel B).

Imidazole also accelerated P_{680}^+ reduction in Mn-depleted wild-type* PSII particles, decreasing the overall half-decay time of P_{680}^+ reduction from approximately 2 μs in the absence of imidazole to approximately 0.8 μs in the presence of 100 mM imidazole (Figure 2A). In the absence of imidazole, the P_{680}^+ reduction kinetics in Mn-depleted wild-type* PSII particles could be fit with four exponentially decaying phases:[2] 51 ± 1% with 0.38 ± 0.03 μs, 21 ± 3% with 4.7 ± 0.2 μs, 22 ± 1% with 82 ± 6 μs, and 7 ± 2% with ≥1 ms. The addition of imidazole caused the ≈0.4 and ≈4.7 μs phases to increase at the expense of the ≈82 μs phase and accelerated both the ≈4.7 and ≈82 μs phases. In the presence of 100 mM imidazole, the P_{680}^+ reduction kinetics could be fit as follows:[2] 62 ± 2% with 0.38 ± 0.07 μs, 31 ± 2% with 2.3 ± 0.4 μs, 4.2 ± 0.6% with 24 ± 9 μs, and 3.5 ± 0.2% with ≥1 ms. The rates of the ≈4.5 and ≈82 μs phases increased hyperbolically with imidazole concentration, reaching limiting rate constants of $(2.0 \pm 0.1\ \mu s)^{-1}$ and $(17 \pm 2\ \mu s)^{-1}$, respectively, and achieving half-saturation at 27 ± 7 mM imidazole (not shown).

Q_A^- Oxidation. The flash-induced formation of Q_A^-, as monitored at 325 nm, is presented in Figure 3. At this wavelength, P_{680}^+ (*87*, *88*) and $Y_Z^\bullet$ (*87*, *88*, *91*−*94*) make only minor contributions to the absorbance changes. In Mn-depleted wild-type* PSII particles (Figure 3A), Q_A^- was stable on the time scale of these measurements, ultimately being oxidized by potassium ferricyanide or $Y_Z^\bullet$ (*87*, *88*, *91*). In Y161F PSII particles (Figure 3B) and in all of the His190 mutants (e.g., Figure 3C−F), the majority of Q_A^- decayed rapidly, presumably by reducing P_{680}^+. In all of the His190 mutants except H190E, the fractions of rapidly decaying Q_A^- decreased substantially in the presence of 5−100 mM imidazole (Figure 3C−E). Presumably, Q_A^- reduces P_{680}^+ in fewer reaction centers in these mutants in the presence of

[2] The exponentially decaying phases are reported in terms of initial amplitudes (% of total) and lifetimes (i.e., k^{-1}), that is, the time required for the amplitude to decay to 1/e of its initial value. The r^2 values for the fits of the 810 nm data ranged from 0.98 to greater than 0.99 for all concentrations of imidazole.

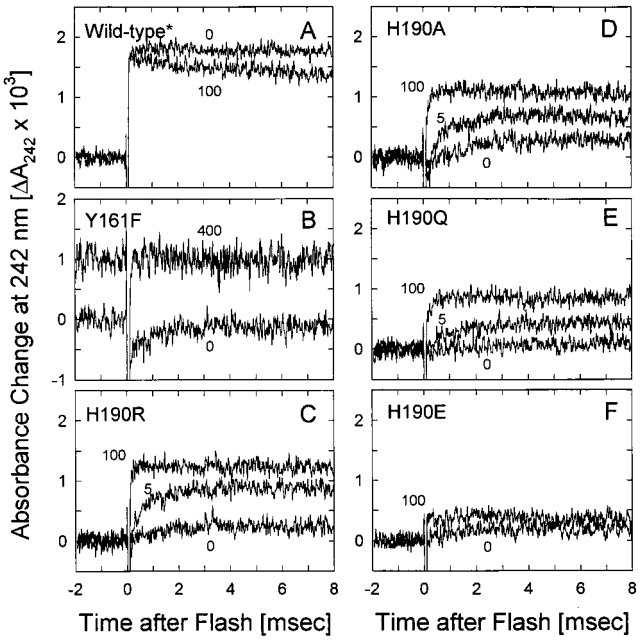

FIGURE 4: Formation of $Y_Z^{\bullet}$ in isolated PSII particles in the presence of 0, 5, 100, and 400 mM imidazole, as monitored at 242 nm: (A) Mn-depleted wild type*, (B) Y161F, (C) H190R, (D) H190A, (E) H190Q, and (F) H190E. In panel B, the Y161F trace obtained in the presence of 400 mM imidazole has been shifted upward for clarity. Conditions were as follows: 16 μg of Chl in 0.9 mL of 20 mM TES, 0.04% *n*-dodecyl β-D-maltoside, 10 μM $K_3Fe(CN)_6$, pH 7.5, and 21 °C. Samples were incubated in darkness for 2 min before the monitoring beam was turned on. Red-filtered xenon flashes (4 μs fwhm) were applied at 10 s intervals. The wild-type* and His190 mutant traces each represent the average of 576 sweeps. The Y161F traces each represent the average of 1296 sweeps. Samples were replaced after every 144 sweeps. The Chl/Q_A ratios for the wild-type*, Y161F, H190R, H190A, H190Q, and H190E PSII particles were 54, 39, 50, 58, 51, and 86, respectively.

imidazole. Imidazole also decreased the fraction of rapidly decaying Q_A^- in H190E PSII particles, but the effect was less pronounced (Figure 3F). The data of Figure 3C−F are an additional indication that Y_Z oxidation is impaired in the His190 mutants and that imidazole partly compensates for the loss of the His190 imidazole moiety.

Y_Z Oxidation. The flash-induced formation of $Y_Z^{\bullet}$, as monitored at 242 nm, is shown in Figure 4. This wavelength is nearly isosbestic for both Q_A^- and P_{680}^+ (*87*, *88*, *92*). As expected, Mn-depleted wild-type* PSII particles showed a significant flash-induced absorbance increase at this wavelength (Figure 4A), whereas Y161F PSII particles, which lack Y_Z, showed no increase, both in the absence and in the presence of 0.4 M imidazole (Figure 4B). This absence of a flash-induced absorbance increase at 242 nm is expected for a mutant that lacks Y_Z. In contrast to Y161F, all of the His190 mutant PSII particles showed some $Y_Z^{\bullet}$ formation, but the extent of $Y_Z^{\bullet}$ formation was far less than that of the wild type* (e.g., Figure 4C−F). In all of the His190 mutants except H190E, the extent of $Y_Z^{\bullet}$ formation increased dramatically in the presence of 5−100 mM imidazole (e.g., Figure 4C−E). Imidazole also increased the extent of $Y_Z^{\bullet}$ formation in H190E PSII particles, but to a lesser extent (Figure 4F).

In the absence of imidazole, Y161F PSII particles showed a flash-induced absorbance decrease that decayed with a rate comparable to P_{680}^+ reduction and Q_A^- oxidation in this mutant (lower trace of Figure 4B; cf. Figures 1B and 3B). This decay was accelerated dramatically in the presence of 400 mM imidazole (upper trace of Figure 4B). Because the addition of 400 mM imidazole also dramatically accelerated P_{680}^+ reduction in this mutant (Figure 2B) but had little effect on Q_A^- oxidation (Figure 3B), we attribute the rising decay in Y161F PSII particles in the absence of imidazole (lower trace of Figure 4B) to the reduction of P_{680}^+. Consistent with previous measurements (*88*), no flash-induced absorbance changes were observed at 240 nm in Y161F PSII particles (not shown). On the basis of absorbance measurements acquired at several wavelengths between 239 and 245 nm, we propose that the spectrum of $P_{680}^+ - P_{680}$ is isosbestic at 240 nm in Y161F PSII particles and near 242 nm in the His190 mutants, implying that the absorbance spectrum of $P_{680}^+ - P_{680}$ in the UV is shifted in Y161F compared to that for His190 mutant PSII particles. However, a definitive statement will require the acquisition of full $P_{680}^+ - P_{680}$ absorbance spectra. The $P_{680}^+ - P_{680}$ absorbance spectrum from 400 to 450 nm is essentially the same in Y161F and wild-type PSII particles (B. A. Diner, personal communication).

The rate of $Y_Z^{\bullet}$ formation also increased dramatically in His190 mutant PSII particles as the concentration of imidazole was increased from 0 to 100 mM (e.g., Figure 4C−E). This increase is expected because the rate of Y_Z oxidation corresponds to the sum of the intrinsic rate constants, $k_Z + k_Q + k_X$; an increased extent of $Y_Z^{\bullet}$ formation implies an increase in k_Z. The data of Figure 4 show directly that Y_Z oxidation is impaired in the His190 mutants and that imidazole partly compensates for the loss of the His190 imidazole moiety.

Estimation of Rate Constants k_Z and k_Q in the His190 and Y161F Mutants. The intrinsic rate constants for the His190 and Y161F mutants in the presence of 0, 5, and 100 mM imidazole were calculated from the data obtained at 432.5, 325, and 242 nm (e.g., Figures 1, 3, and 4, respectively). The sum $k_Z + k_Q + k_X$ was obtained from data acquired at 432.5 nm (e.g., Figure 1). In principle, this sum can be obtained at any of the three wavelengths because the three intrinsic rate constants represent parallel reactions. However, the signal-to-noise ratio was better at 432.5 nm. Also, the $k_Z + k_Q + k_X$ values were obtained at 432.5 nm rather than at 810 nm because significantly more data were acquired at 432.5 nm. Nevertheless, values obtained from individual traces acquired at 810 nm were consistent with those obtained at 432.5 nm within 25% (e.g., see below, Figure 8).

The absorbance decays at 432.5 nm could be fit with the sum of two exponentially decaying phases.[3] The faster phase dominated (60−70% of the total decay in all mutants) and was used as an estimate of $k_Z + k_Q + k_X$ (Table 1). The rate of this phase increased with imidazole concentration, but its extent remained essentially constant. The absorbance decays at 325 nm (e.g., Figure 3) could be fit with the sum of two exponentially decaying phases plus an offset.[4] The value of $k_Z + k_Q + k_X$ determined at 432.5 nm could be

[3] In the absence of imidazole, the r^2 values for the fits of the 432.5 nm data ranged from 0.98 to greater than 0.99. In the presence of 100 mM imidazole, the r^2 values ranged from 0.96 to 0.98 in all mutants except H190R and H190S, where the values were 0.90 and 0.89, respectively.

Table 1: Estimation of Rate Constants k_Z and k_Q in His190 Mutant and Y161F PSII Particles at pH 7.5 in the Presence of 0 and 100 mM Imidazole

	0 mM imidazole			100 mM imidazole			
mutant	$k_Z + k_Q + k_X$[a] (s^{-1}) (±3%)	k_Z[b] (s^{-1}) (±25%)	k_Q[c] (s^{-1}) (±7%)	$k_Z + k_Q + k_X$[a] (s^{-1}) (±10%)	k_Z[b] (s^{-1}) (±15%)	k_Q[c] (s^{-1}) (±17%)	$k_Z(100)/k_Z(0)$ (-fold) (±30%)
H190A	870	160	680	6830	4640	2050	29
H190Q	760	40	550	7340	3460	2480	87
H190R	1040	130	760	10900	7120	3150	55
H190E	1350	230	980	3070	1130	1590	5
H190G	770	50	640	3100	1300	1480	26
H190K	1000	250	640	6980	4030	2500	16
H190S	1040	60	720	13300	4920	3880	82
Y161F	1240	0	870	1330	0	950	−

[a] Obtained from data acquired at 432.5 nm (see Figure 1 and the text). [b] Calculated from the relation $k_Z/(k_Z + k_Q + k_X)$, obtained from data acquired at 242 nm (e.g., Figure 4) relative to the wild type* and normalized to the Chl/Q_A ratio of the wild type*. The Chl/Q_A ratios were 54, 58, 51, 50, 86, 58, 64, 39, and 39 for the wild-type*, H190A, H190Q, H190R, H190E, H190G, H190K, H190S, and Y161F PSII particles, respectively. [c] Calculated from the relation $k_Q/(k_Z + k_Q + k_X)$, obtained from data acquired at 325 nm (see Figure 3 and the text).

used in fitting the 325 nm data without changing the quality of the fits. The sum of the amplitudes of the exponentially decaying phases divided by the total ΔA_{325} provided the ratio $k_Q/(k_Z + k_Q + k_X)$, that is, the fraction of Q_A^- that was oxidized by P_{680}^+. The data acquired at 242 nm (e.g., Figure 4) provided the ratio $k_Z/(k_Z + k_Q + k_X)$, that is, the fraction of $Y_Z^\bullet$ that was formed after a single flash. For each His190 mutant, the ratio $k_Z/(k_Z + k_Q + k_X)$ in the presence of 0, 5, and 100 mM imidazole was obtained by dividing the ΔA_{242} obtained 8 ms after the actinic flash by the corresponding ΔA_{242} in Mn-depleted wild-type* PSII particles in the absence of imidazole (Figure 4A). The ratio was corrected for differences in Chl/Q_A ratios between mutant and wild-type* particles (see Table 1).

The values of k_Z and k_Q estimated for all seven His190 mutants and Y161F PSII particles in the presence of 0 and 100 mM imidazole are presented in Table 1. In the presence of 0 mM imidazole, the rate of P_{680}^+ reduction appeared to be dominated by k_Q in all mutants. The range of k_Q values (550−980 s^{-1}) corresponds to half-decay times of 0.7−1.3 ms. Similar half-decay times for the reduction of P_{680}^+ by Q_A^- have been reported in PSII particles from the Y161F mutant of *Synechocystis* 6803 [0.8−1.0 ms (*84*, *88*)], in spinach PSII membranes that had been subjected to strong irradiance to destroy Y_Z [0.7−0.8 ms (*100*)], and in Mn-depleted PSII particles from pea at pH 4 (conditions where electron donation from Y_Z to P_{680}^+ is postulated not to occur in a majority of reaction centers) [870 μs (*32*)]. The value of k_Z varies considerably in the His190 mutants. However, there appears to be no correlation between k_Z and the nature of the residue substituted for His190 (e.g., k_Z is smallest in H190Q, H190G, and H190S PSII particles, intermediate in H190A and H190R PSII particles, and greatest in H190E and H190K PSII particles). The values for k_Z (40−250 s^{-1}) correspond to half-decay times of 2.8−17 ms compared to a half-decay time of approximately 2 μs for Mn-depleted wild-type* PSII particles at this pH value (Figure 2A). In the wild-type* particles, P_{680}^+ reduction should be dominated by k_Z. Therefore, at pH 7.5, the rate of electron transfer from Y_Z to P_{680}^+ is slowed 1400−8500-fold in the absence of the His190 imidazole moiety, depending on the mutant.

In the presence of 5 mM imidazole, k_Z increased 4−8-fold in all His190 mutants except H190K (2.5-fold) and H190E (1.5-fold), while k_Q increased by at most 30−40% (not shown). In the presence of 100 mM imidazole, k_Z increased dramatically (26−87-fold) in all His190 mutants except H190K (16-fold) and H190E (5-fold), while k_Q increased to lesser extents (1.6−5-fold in all His190 mutants). The dramatic increases of k_Z in most His190 mutants in the presence of 5−100 mM imidazole confirm that imidazole accelerates Y_Z oxidation in the absence of the His190 imidazole moiety. The increase of k_Q in the presence of 100 mM imidazole is not understood. It could arise from an effect of imidazole on the environment(s) of P_{680} and/or Q_A, the latter via the non-heme iron or Q_B sites. Note, however, that 100 mM imidazole has little effect on k_Q in Y161F PSII particles.

Other Bases. Histidine, 4-methylimidazole, 2-methylimidazole, 1-methylimidazole, TRIS, methylamine, and ethanolamine also accelerated P_{680}^+ reduction in H190A PSII particles, as monitored at 432.5 and 810 nm (Figure 5). Because of their high pK_a values (pK_a = 10.6 and 9.5, respectively), methylamine and ethanolamine were compared to Mn-depleted wild-type* PSII particles at pH 9.5 rather than at pH 7.5 (Figure 5C,F). Neither pyridine (100 mM) nor urea (100 mM) had any effect of P_{680}^+ reduction in Y161F or H190A PSII particles (not shown). [The urea (pK_a = 0.18) was employed to determine if the effect of 100 mM imidazole on Y161F and H190A PSII particles was the result of a nonspecific denaturing effect of the imidazole.]

$Y_Z^\bullet$ Reduction. The reduction of $Y_Z^\bullet$ after a flash, as monitored at 242 nm, is presented in Figure 6 for Mn-depleted wild-type* and H190A PSII particles. Note the very different absorbance scales for the mutant and wild type. In the Mn-depleted wild-type* particles, the half-decay time for $Y_Z^\bullet$ reduction (≈0.46 s) corresponded closely to that expected for charge recombination between Q_A^- and $Y_Z^\bullet$ in Mn-depleted PSII preparations at pH 7.5 (*91*) and showed the same acceleration at lower pH values (not shown). As expected on the basis of the data presented earlier (Figure 4), the extent of $Y_Z^\bullet$ formation in H190A PSII particles increased with imidazole concentration (Figure 6A,D−F).

[4] In the absence of imidazole, the r^2 values for the fits of the 325 nm data ranged from 0.98 to greater than 0.99 for all mutants except H190E, where the value was 0.95. In the presence of 100 mM imidazole, the r^2 values ranged from 0.84 to 0.93 in all mutants except Y161F, H190S, and H190Q, where the values were 0.97, 0.80, and 0.79, respectively.

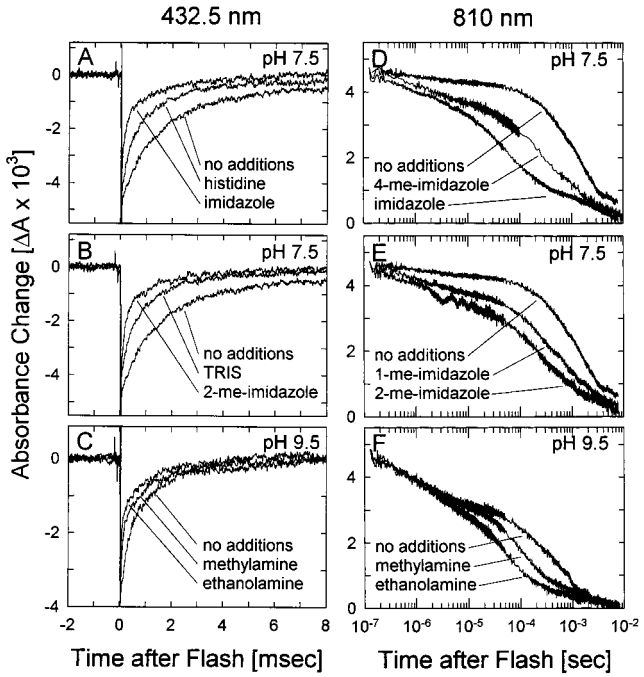

FIGURE 5: Formation and decay of P_{680}^+ in H190A PSII particles in the presence of 100 mM concentrations of various exogenous bases, as monitored at 432.5 (left panels) and 810 nm (right panels). Note the logarithmic time scale employed in the right panels. Conditions were as follows: same as in Figure 1 for panels A and B, same as in Figure 2 for panels D and E, and same as in Figures 1 and 2 for panels C and F, respectively, except that the buffer contained 20 mM CHES (pH 9.5) instead of TES.

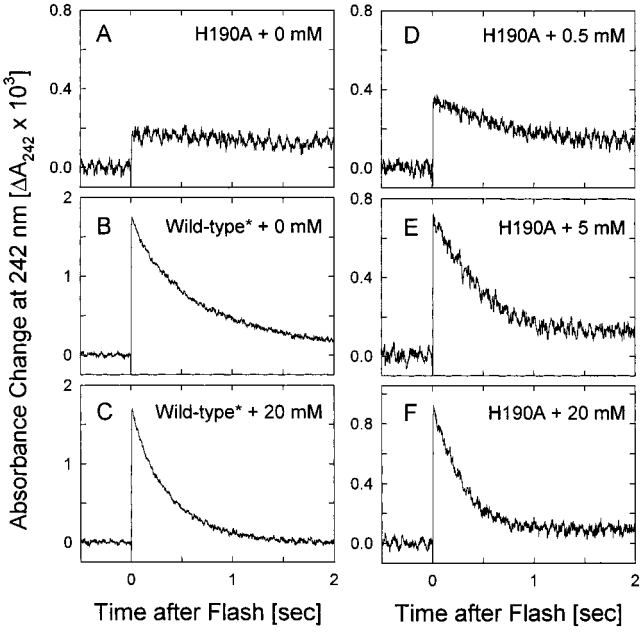

FIGURE 6: Formation and reduction of $Y_Z^\bullet$ in H190A and wild-type* PSII particles in the absence and presence of imidazole, as measured at 242 nm: (A and D−F) H190A PSII particles in the presence of 0, 0.5, 5, and 20 mM imidazole, respectively, and (B and C) wild-type* PSII particles in the presence of 0 and 20 mM imidazole, respectively. Conditions were the same as in Figure 4 except that samples were given 10 preflashes at 10 s intervals to ensure oxidation of Y_D prior to data collection. Each wild-type* trace represents the average of 16 sweeps. Each H190A trace represents the average of 64 sweeps. Note the very different vertical scales for the wild-type* and H190A samples. Note also that the time scale is very different from that in Figures 1−5.

The subsequent decay of $Y_Z^\bullet$ was substantially slower than that in wild-type* PSII particles (compare panels A and B of Figure 6). This was true in all His190 mutants examined (H190A, H190Q, H190R, and H190G). In all of these mutants, the decay of $Y_Z^\bullet$ accelerated dramatically in the presence of 0.5−5 mM imidazole (e.g., Figure 6A,D−F) and other bases [4-methylimidazole, 2-methylimidazole, and 1-methylimidazole (not shown)]. Indeed, in the presence of 5 mM imidazole, the rate of $Y_Z^\bullet$ reduction in H190A particles was comparable to that of Mn-depleted wild-type particles in the absence of imidazole (compare panels B and E of Figure 6). Similar concentrations of imidazole also accelerated $Y_Z^\bullet$ reduction in Mn-depleted wild-type* particles (compare panels B and C of Figure 6). Indeed, comparable rates of $Y_Z^\bullet$ reduction were observed in H190A and Mn-depleted wild-type* particles in the presence of 20 mM imidazole (compare panels C and F of Figure 6). The data of Figure 6 show that imidazole and other small organic bases, in addition to accelerating the oxidation of Y_Z, also accelerate the reduction of $Y_Z^\bullet$ in His190 mutant and Mn-depleted wild-type* PSII particles.

Mechanism of Action of Imidazole and Other Bases. To determine if small organic bases, such as imidazole, exchange slowly or rapidly into the vicinity of Y_Z, a sample of H190A PSII particles was incubated for 2 min in the presence of 0.1 M imidazole at twice the usual Chl concentration (i.e., at 18 μg of Chl/mL). Then, one aliquot was analyzed in a 5 mm path length cuvette (Figure 7, trace labeled Before Column), and the remainder was passed rapidly through a Pharmacia HR 10/10 Fast Desalting Column. The eluted sample, analyzed in a 10 mm path length cuvette immediately after being eluted from the column (Figure 7, trace labeled

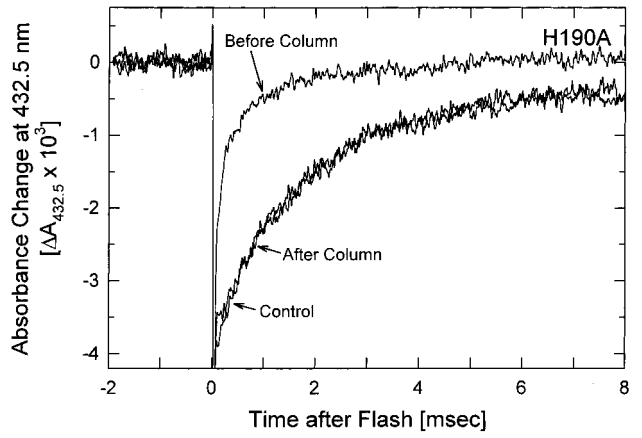

FIGURE 7: Effect on P_{680}^+ reduction kinetics of rapidly removing 100 mM imidazole from H190A PSII particles. (Before Column) PSII particles were incubated for 2 min in the presence of 100 mM imidazole at twice the normal reaction center concentration and then analyzed in a 5 mm path length cuvette. (After Column) PSII particles were analyzed in a 10 mm path length cuvette immediately after elution from a Pharmacia HR 10/10 Fast Desalting Column. (Control) The PSII sample was incubated in the absence of imidazole and analyzed in a 10 mm path length cuvette. The individual traces were normalized to their initial amplitudes. Conditions were the same as in Figure 1.

After Column), was indistinguishable from a control sample incubated in the absence of imidazole (Figure 7, trace labeled Control). This result shows that imidazole (and presumably other small organic bases) exchanges rapidly into (and out of) the vicinity of Y_Z in H190A particles. (We used different

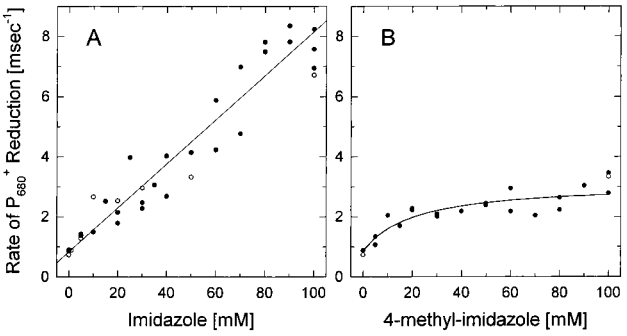

FIGURE 8: Rate constant of P_{680}^+ reduction in H190A PSII particles as a function of the concentration of (A) imidazole and (B) 4-methylimidazole: (●) the dominant exponentially decaying phase measured at 432.5 nm and (○) the dominant exponentially decaying phase measured at 810 nm. The solid line in panel A is a least-squares fit to the filled circles (with an r^2 value of 0.93), corresponding to a rate constant of $(7.4 \pm 0.7) \times 10^4$ M^{-1} s^{-1}. The solid line in panel B is a fit to the filled circles (with an r^2 value of 0.74) with a limiting rate constant of $(3.1 \pm 0.3) \times 10^3$ s^{-1} and a half-saturation concentration of 21 ± 9 mM. Conditions were the same as in Figures 1 and 2.

path length cuvettes to analyze the Before Column and After Column samples to compensate for the expected 2-fold dilution of the sample during chromatography.)

To determine if imidazole or other small organic bases bind to a specific site near Y_Z, the rate of P_{680}^+ reduction was measured in H190A PSII particles in the presence of various concentrations of imidazole and other bases. Data were acquired at both 432.5 and 810 nm. The rates of the dominant exponentially decaying phases were plotted as a function of the concentration of base (at all concentrations of base, the dominant phase corresponded to 60−70% of the total decay at 432.5 nm and 50−60% at 810 nm). For imidazole (Figure 8A) and 2-methylimidazole (not shown), the rate increased linearly up to a concentration of 100 mM, showing no hint of saturation. These results are consistent with a second-order process characterized by a rate constant of $(7.4 \pm 0.7) \times 10^4$ M^{-1} s^{-1} for imidazole (obtained from the straight line in Figure 8A) and $(5.0 \pm 0.6) \times 10^4$ M^{-1} s^{-1} for 2-methylimidazole (not shown). These constants increased to $(9.3 \pm 0.9) \times 10^4$ and $(1.1 \pm 0.1) \times 10^5$ M^{-1} s^{-1}, respectively, when they were corrected for the amount of base that is unprotonated at pH 7.5 ($pK_a = 6.9$ for imidazole and $pK_a = 7.6$ for 2-methylimidazole). Similar second-order rate constants have been reported for the reduction of $Y_Z^\bullet$ by neutral ascorbic acid ($1.4-4.0 \times 10^4$ M^{-1} s^{-1}) and hydroquinone (2.5×10^5 M^{-1} s^{-1}) (*101*, *102*), although higher second-order rate constants have been reported for the reduction of $Y_Z^\bullet$ by benzidine [$1.3-3.2 \times 10^6$ M^{-1} s^{-1} (*101*)] and Mn^{2+} [$0.6-4.8 \times 10^7$ M^{-1} s^{-1} (*103*, *104*)]. In contrast, for 4-methylimidazole (Figure 8B), the rate appeared to reach a limiting value. The solid line in Figure 8B represents a hyperbolic fit with a limiting rate constant of $(3.1 \pm 0.3) \times 10^3$ s^{-1} and a half-saturation concentration of 21 ± 9 mM. Similar data, albeit with lower limiting rate constants, were obtained with 1-methylimidazole, histidine, and TRIS (not shown). There was no correlation between these limiting rate constants and the pK_a values of the added bases ($pK_a = 7.5$, 7.2, 6.0, and 8.3 for 4-methylimidazole, 1-methylimidazole, histidine, and TRIS, respectively).

DISCUSSION

In all seven D1-His190 mutants examined, the rates of P_{680}^+ reduction, Y_Z oxidation, and $Y_Z^\bullet$ reduction were slowed dramatically, and the rate of Q_A^- oxidation was accelerated to values consistent with the reduction of P_{680}^+ by Q_A^- rather than by Y_Z. There appeared to be no correlation between these rates and the structure of the residue substituted for His190. Calculations of k_Z and k_Q from data acquired at 432.5, 325, and 242 nm showed that, in all seven His190 mutants, P_{680}^+ reduction is dominated by k_Q. These calculations also show that k_Z, the rate of oxidation of Y_Z by P_{680}^+, is slowed by factors of 1400−8500.

A previous study of the D1-H190Q and H190D mutants of *Synechocystis* 6803 (cited in refs *48*, *50*, and *51*) reported that k_Z was slowed only 200-fold compared to that for wild-type PSII particles. No details were provided, but the measurements (at 432.5 and 325 nm and other wavelengths) were conducted at pH 9.0 (B. A. Diner, personal communication). Importantly, the initial data point of P_{680}^+ decay after a flash (measured at 432.5 nm) was acquired ≈1 μs after the actinic flash. These measurements yielded an overall half-decay time of ≈12 μs for Mn-depleted wild-type PSII particles (B. A. Diner, personal communication). In contrast, our initial data point for P_{680}^+ decay (measured at 810 nm) was acquired 130 ns after the actinic flash, yielding an overall half-decay time of ≈2 μs for Mn-depleted wild-type* PSII particles (Figure 2A). However, if we take the ΔA_{810} value at 1 μs to be our initial data point (Figure 2A), then the half-decay time in our Mn-depleted wild-type* particles becomes ≈15 μs and the difference between our wild-type* and mutant k_Z values decreases to 190−1100-fold. Therefore, the mutant k_Z values calculated in this study and in the previous study may not differ significantly. In any case, whether k_Z is slowed 200-fold [as stated previously (*48*, *50*, *51*)] or 1400−8500-fold (as determined in this study), the principal conclusion remains the same: the oxidation of Y_Z by P_{680}^+ is slowed dramatically in the absence of the His190 imidazole moiety.

In six of the seven His190 mutants examined, the rates of P_{680}^+ reduction, Y_Z oxidation, and $Y_Z^\bullet$ reduction were accelerated dramatically in the presence of imidazole and other small organic bases. Significant accelerations of $Y_Z^\bullet$ reduction were observed even in the presence of 0.5 mM imidazole, while significant accelerations of P_{680}^+ reduction and Y_Z oxidation were observed in the presence of 5 mM imidazole. In other chemical complementation studies, partial restoration of histidine function has typically been observed in the presence of 0.5−50 mM imidazole (*66*, *68*−*70*, *72*, *105*, *106*). Calculations of k_Z and k_Q values from data acquired at 432.5, 325, and 242 nm showed that, in the presence of 100 mM imidazole, k_Z increased 26−87-fold in all His190 mutants except H190K and H190E, where the increase was 16- and 5-fold, respectively. The much smaller increase of k_Z in H190E PSII particles is not understood. Note, however, that the H190E mutation places two glutamate residues close together (i.e., Glu189 and Glu190).

The severe disruption of the normal electron transfer reactions of Y_Z in all seven His190 mutants shows that D1-His190 plays a pivotal role in Y_Z function. The partial restoration of rapid P_{680}^+ reduction, Y_Z oxidation, and $Y_Z^\bullet$ reduction by imidazole and other bases shows that these bases

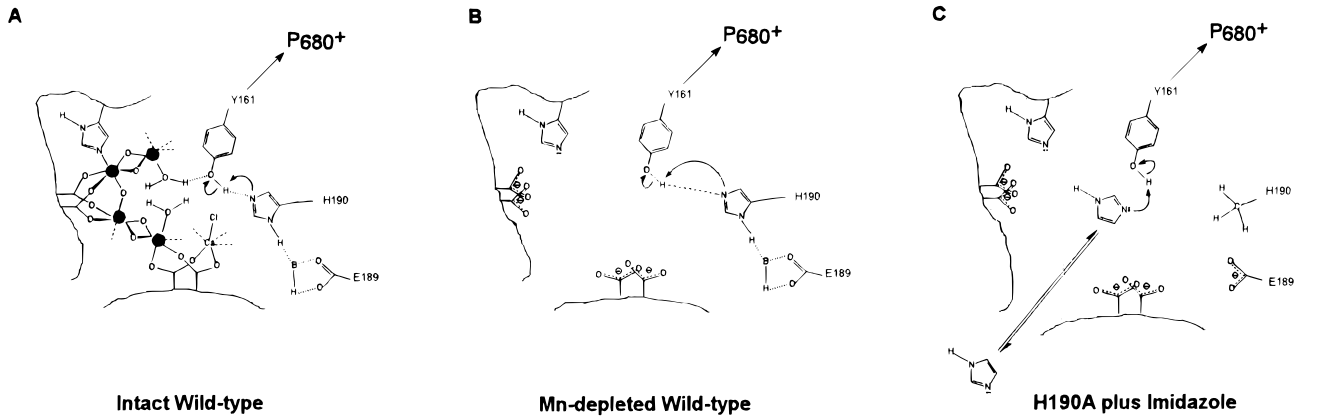

FIGURE 9: Proposed structures of the environment of Y_Z (Y161 of the D1 polypeptide) in (A) intact, O_2-evolving wild-type PSII reaction centers (figure modified from ref *18*), (B) Mn-depleted wild-type PSII reaction centers, and (C) H190A mutant PSII reaction centers. Single arrows depict electron movements. In these models, D1-His190 is the proton acceptor for Y_Z. The unidentified proton acceptor for the distal proton of His190 is depicted as B and is shown being positioned by D1-Glu189. In panel B, the suboptimal interaction between Y_Z and His190 is depicted as a lengthening of the hydrogen bond. In panel C, an exogenous imidazole molecule is depicted as diffusing to Y_Z through a small-diameter pore or channel and replacing the function of the absent His190 imidazole moiety.

are able to partly replace the function of the His190 imidazole moiety, presumably by forming a hydrogen bond with the hydroxyl proton of Y_Z or with the phenolic oxygen of $Y_Z^\bullet$. We conclude that D1-His190 is the proton acceptor for Y_Z, just as D2-His189 is the proton acceptor for Y_D (*28*) (also see refs *27* and *47*−*49*). This conclusion is consistent with previous studies showing that the redox properties of Y_Z in Mn-depleted preparations are strongly influenced by a nearby group with a pK_a value of 6−8 (*32*, *41*, *99*, *107*). It is also consistent with a recent proposal, based on FTIR studies, that both Y_Z and $Y_Z^\bullet$ form a hydrogen bond with a histidine residue (*108*). This conclusion is illustrated schematically in Figure 9, which compares the proposed environments of Y_Z in intact wild-type, Mn-depleted wild-type, and H190A mutant reaction centers. Recent evidence consistent with our conclusion that D1-His190 is the proton acceptor for Y_Z has been provided by pulsed ENDOR studies of $Y_Z^\bullet$ in globally ^{15}N-labeled, Mn-depleted, PSII particles from *Synechocystis* 6803 that lack Y_D (K. Campbell, B. A. Diner, and R. D. Britt, personal communication). These studies show the existence of a weak isotropic ^{15}N coupling to $Y_Z^\bullet$. This coupling is consistent with a hydrogen bond between $Y_Z^\bullet$ and a nitrogen atom that is weaker or more disordered than the hydrogen bond observed (*28*) between $Y_D^\bullet$ and the τ-nitrogen of D2-His189.

In contrast to our conclusion that D1-His190 is the proton acceptor for Y_Z, two previous studies reached the opposite conclusion. The first study examined the EPR line shapes of $Y_Z^\bullet$ in PSII membranes isolated from the D1-H190F and H190Y mutants of *Chlamydomonas reinhardtii* (*53*). Because these line shapes were similar to those of $Y_Z^\bullet$ in wild-type membranes (*53*), the presence of a hydrogen bond between $Y_Z^\bullet$ and D1-His190 was thought to be improbable (*53*). [Similar data were obtained with PSII particles from the D1-H190Q (*48*, *77*), H190D (*48*), and H190E (*48*) mutants of *Synechocystis* 6803 and were interpreted in a similar fashion (*51*)]. The reasoning was based on the altered EPR line shapes of $Y_D^\bullet$ that have been observed in D2-His189 mutants (*27*, *47*, *48*). The strong hydrogen bond between D2-His189 and $Y_D^\bullet$ is absent in these mutants (*27*, *28*, *47*−*49*). Its absence was thought to be responsible for the altered EPR line shapes (*47*, *51*, *53*). However, recent studies have shown that the spin density distributions of tyrosine radicals in proteins depend only very weakly on the hydrogen bonding status of the radical's phenolic oxygen (*12*, *109*, *110*). Therefore, factors other than the absence of a hydrogen bond to $Y_D^\bullet$ are responsible for the altered EPR line shapes in the D2-His189 mutants. These results show that the normal line shapes of $Y_Z^\bullet$ in the D1-His190 mutants do not eliminate D1-His190 as the proton acceptor for Y_Z.

A second study concluded that D1-His190 is not the proton acceptor for Y_Z on the basis of light-minus-dark FTIR difference spectra (*77*). These spectra were obtained with D1-H190Q and Mn-depleted wild-type PSII particles from *Synechocystis* 6803. If D1-His190 becomes protonated in the presence of $Y_Z^\bullet$, then the light-minus-dark difference spectrum of $Y_Z^\bullet$ and its environment should differ significantly between H190Q and wild-type PSII particles. Because little or no differences were found, the authors concluded that D1-His190 is not the proton acceptor for Y_Z (*77*). However, the dominant feature in these spectra (outside the amide region) was a positive band near 1478 cm^{-1}. Depending on the illumination and dark adaptation conditions, this band was attributed either to the ν(C−O) vibrational mode of $Y_Z^\bullet$ or to the sum of the ν(C−O) vibrational modes of $Y_Z^\bullet$ and $Y_D^\bullet$ (*77*). However, there is compelling evidence that the 1478 cm^{-1} band corresponds to the ν(C−O) vibrational mode of Q_A^- (*111*−*115*) (also see refs *116*−*118*). Furthermore, evidence that the ν(C−O) vibrational modes of $Y_D^\bullet$ and $Y_Z^\bullet$ occur near 1503 (*29*, *49*, *114*) and 1512 cm^{-1} (*108*), respectively, now seems conclusive. Some of the most recent evidence is based on unambiguous spectral shifts observed in samples that were specifically ^{13}C-labeled at the ring C4 of tyrosine (*29*, *49*, *108*). Therefore, as pointed out by others (*29*, *49*, *108*, *114*), it seems likely that the light-minus-dark FTIR difference spectra reported in ref *77* are dominated by contributions from Q_A^- and its environment.[5]

[5] The authors of two recent publications continue to maintain that the 1478 cm^{-1} band corresponds to the ν(C−O) modes of $Y_Z^\bullet$ and/or $Y_D^\bullet$ (*137*, *138*). However, the data acquired with ^{13}C-ring-C4-labeled tyrosine in these publications show no unambiguous spectral shifts. Furthermore, the EPR data that are presented to rule out a contribution of Q_A^- to the 1478 cm^{-1} band were acquired under illumination conditions different from those used to acquire the FTIR data.

These contributions may have obscured contributions associated with the protonation of D1-His190 in the presence of $Y_Z^{\bullet}$. Therefore, the data of ref *77* do not rule out D1-His190 as the proton acceptor for Y_Z.

Imidazole appears to rapidly exchange into (and out of) the vicinity of Y_Z. We presume that other small organic bases behave similarly. In the range of 0−100 mM, imidazole and 2-methylimidazole accelerated P_{680}^+ reduction with apparent second-order rate constants of $(9.3 \pm 0.9) \times 10^4$ and $(1.1 \pm 0.1) \times 10^5$ M^{-1} s^{-1}, respectively [after correcting for the amount of base that is unprotonated at pH 7.5 (Figure 8A)]. These rate constants are far lower than expected for diffusional processes (*119*). Therefore, the access of imidazole and 2-methylimidazole to Y_Z must be limited sterically. In contrast, the accelerations of P_{680}^+ reduction by 4-methylimidazole, 1-methylimidazole, histidine, and TRIS showed hyperbolic dependencies on base concentration, with half-saturation concentrations of ≈20 mM and limiting rate constants of at most $(3.1 \pm 0.3) \times 10^3$ s^{-1} (Figure 8B).

Presumably because of their structures, 4-methylimidazole, 1-methylimidazole, histidine, and TRIS have less access to Y_Z than imidazole and 2-methylimidazole. Perhaps imidazole and 2-methylimidazole reach Y_Z via a small-diameter channel. Because of steric hindrance, the passage of the other bases through this channel may be rate-limited by the reorientation of one or more amino acid side chains. This type of "gated entry" is believed to govern the incorporation of Cu^{2+} into apoplastocyanin (*120*) and apoazurin (*121*); in both proteins, the entry of Cu^{2+} into its binding site is believed to be rate-limited by the reorientation of a specific histidine residue.[6] The rate of entry shows a hyperbolic dependence on Cu^{2+} concentration that was explained as a two-step process involving rapid binding of Cu^{2+} to the apoprotein followed by the rate-limiting conformational change that permits entry into the Cu^{2+} site (*122*). The putative channel leading to Y_Z appears to be more constricted in the presence of the D1-His190 imidazole moiety because, in Mn-depleted wild-type* PSII particles, the acceleration of P_{680}^+ reduction by imidazole also shows a hyperbolic dependence on base concentration (Figure 2A).

Because the oxidation of Y_Z is severely impaired in the absence of D1-His190, we conclude that rupture of the O−H bond of Y_Z is rate-limiting for electron transfer from Y_Z to P_{680}^+, at least in the absence of the Mn cluster. The same conclusion has been reached by others on the basis that, in Mn-depleted preparations, electron transfer from Y_Z to P_{680}^+ is pH-dependent (*41*) and exhibits a significant deuterium isotope effect (*31*, *32*, *100*, *123*) (however, see the caveat offered in ref *100*). In intact, O_2-evolving PSII preparations, only the S-state-dependent microsecond components of P_{680}^+ reduction exhibit a significant deuterium isotope effect (*124*); no deuterium isotope effect has been observed for the nanosecond components of P_{680}^+ reduction in O_2-evolving PSII preparations (*31*, *32*, *124*, *125*). The absence of a deuterium isotope effect on the nanosecond components of P_{680}^+ reduction in O_2-evolving PSII preparations suggests that the interaction between D1-His190 and Y_Z is optimized for electron transfer in the intact system. The fact that rupture of the O−H bond of Y_Z has become rate-limiting in the absence of the Mn cluster implies that the interaction between D1-His190 and Y_Z is no longer optimal. This suboptimal interaction may explain the higher activation energy for Y_Z oxidation (*32*, *33*, *126*) and the dramatically slower rates of P_{680}^+ reduction (*31*, *32*, *95*−*100*) that have been measured in Mn-depleted preparations compared to those for O_2-evolving preparations despite the >120 mV decrease in the $Y_Z^{\bullet}-Y_Z$ midpoint potential that has been observed in the absence of the Mn cluster (*84*, *127*). Otherwise, the decrease in the $Y_Z^{\bullet}-Y_Z$ midpoint potential in the absence of the Mn cluster would be expected to increase the rate of electron transfer from Y_Z to P_{680}^+ (*128*−*130*).

The fact that imidazole accelerates P_{680}^+ reduction in Mn-depleted wild-type* PSII particles (Figure 2A) is consistent with a suboptimal interaction between D1-His190 and Y_Z. However, the multiexponential decay of P_{680}^+ in Mn-depleted wild-type PSII preparations has been explained recently as reflecting the protonation state of a nearby base with a p*K* of ≈7 (*32*). The main effect of imidazole on Mn-depleted wild-type* particles is the enhancement of the ≈0.4 and ≈4.7 μs components of P_{680}^+ reduction at the expense of the ≈82 μs component (Figure 2A). Perhaps imidazole only accelerates Y_Z oxidation in wild-type reaction centers in which D1-His190 is protonated and, as a result, is unavailable to form a hydrogen bond with Y_Z. In such reaction centers, the normal hydrogen bond between His190 and Y_Z could be replaced by one involving imidazole. Nevertheless, imidazole and other bases also accelerate $Y_Z^{\bullet}$ reduction in Mn-depleted wild-type* PSII particles (Figure 6C). This finding provides further evidence that the interaction between D1-His190 and Y_Z is not optimal in the absence of the Mn cluster. This suboptimal interaction is depicted in Figure 9B as a lengthening of the hydrogen bond between Y_Z and D1-His190.

Because the rate of $Y_Z^{\bullet}$ reduction is slowed dramatically in the His190 mutants (Figure 6A), and because the rate is accelerated to normal rates by imidazole and other bases (Figure 6B−D), we conclude that the hydroxyl proton of Y_Z remains bound to D1-His190 during the lifetime of $Y_Z^{\bullet}$ and that the reprotonation of $Y_Z^{\bullet}$ is rate-limiting for $Y_Z^{\bullet}$ reduction, at least in Mn-depleted PSII particles. Several studies have shown that $Y_Z^{\bullet}$ forms a hydrogen bond with a nearby group in Mn-depleted PSII preparations (*11*, *19*, *24*−*27*). This group must be D1-His190. Therefore, we attribute the dramatically slower rate of $Y_Z^{\bullet}$ reduction in the His190 mutants to the absence of the hydrogen bond between $Y_Z^{\bullet}$ and His190. Imidazole and other organic bases must accelerate $Y_Z^{\bullet}$ reduction in these mutants by donating a proton to the phenolic oxygen of $Y_Z^{\bullet}$.

Several studies have previously concluded that the hydroxyl proton of Y_Z remains bound to the proton acceptor for Y_Z during the lifetime of $Y_Z^{\bullet}$ (*25*, *31*, *32*, *38*, *39*, *41*, *42*) [although only one of these (*41*) identified D1-His190 as the possible base]. This conclusion was reached on the basis of chlorophyll absorbance band shifts that persist throughout the lifetime of $Y_Z^{\bullet}$ (*25*, *32*, *38*, *39*, *41*, *42*). These absorbance changes have been attributed to an electrochromic effect in the absorbance spectrum of P_{680} (*25*) that is caused by the retention of a positive charge (*25*, *32*, *38*, *39*, *41*, *42*) on the protonated base (i.e., on D1-His190) and have been used

[6] We thank G. T. Babcock for bringing this literature to our attention.

(*31*, *32*, *41*) as an argument against models of photosynthetic water oxidation that involve hydrogen atom abstraction (*12*−*18*). However, this positive charge could be dissipated by the deprotonation of the distal nitrogen of D1-His190 (*11*, *41*) followed by subsequent proton transfer events. Furthermore, it has been suggested recently that the chlorophyll absorbance band shifts are not caused by electrochromism (*19*, *20*). Instead, these band shifts have been suggested to be caused by a change in the strength of a hydrogen bond to the 9-keto carbonyl group of a neutral chlorophyll species (e.g., P_{680}) in the presence of $Y_Z^\bullet$ (or $Y_D^\bullet$). These changes in hydrogen bond strengths have been proposed (*19*, *20*) to give rise to the differential bands near 1707 and 1700 cm^{-1} and 1702 and 1698 cm^{-1} that have been observed in the FTIR difference spectra of $Y_Z^\bullet$ (*108*, *115*) and $Y_D^\bullet$ (*29*, *49*, *114*), respectively. Therefore, although we have concluded that the hydroxyl proton of Y_Z remains bound to D1-His190 during the lifetime of $Y_Z^\bullet$, the impact of this conclusion on the hydrogen atom abstraction models for photosynthetic water oxidation (*12*−*20*) remains to be seen.

The crucial influence of D1-His190 on Y_Z function suggests that D2-His189 may similarly influence Y_D. The $Y_D^\bullet$ radical is involved in a well-ordered hydrogen bond (*24*, *26*, *27*, *48*) from the τ-nitrogen of D2-His189 (*28*). This hydrogen bond is absent in the D2-H189Q (*27*, *28*, *48*, *49*), D2-H189L (*48*), and D2-H189D (*48*) mutants of *Synechocystis* 6803 and is probably absent in other D2-His189 mutants as well [e.g., D2-H189Y (*47*)]. As expected, the light-induced yield of $Y_D^\bullet$ in D2-His189 mutants is lower than that in the wild type [e.g., on the basis of EPR measurements, the yield has been reported to be ≈30 (*47*), ≈50 (*48*), or 17% (*131*) compared to that of the wild type in D2-H189L preparations and to be ≈50 (*48*) or 97% (*77*, *131*) compared to that of the wild-type in D2-H189Q preparations]. However, the decay of $Y_D^\bullet$ in these mutants has been reported to be much more rapid than that in the wild type in one study (*47*) and much slower than that in the wild type in another (*131*). In the latter study, the decay of $Y_D^\bullet$ was much slower in H189L than in H189Q (*131*). The reasons for the discrepancy between the two studies are unclear, but thylakoid membranes were used in the former study (*47*) and PSII particles in the latter (*131*). In the more recent study, the light-induced yield of $Y_D^\bullet$ in D2-H189L PSII particles (measured by EPR) increased from 17 to 38% (compared to that for the wild type) in the presence of imidazole and from 17 to 27% in the presence of 4-methylimidazole (*131*). In addition, the decay of $Y_D^\bullet$ was accelerated significantly in the presence of either compound, but more so in the presence of imidazole than 4-methylimidazole (*131*). These observations suggest that Y_D and Y_Z share a common proton-coupled electron transfer mechanism. However, the accessibility of imidazole to $Y_D^\bullet$ in the recent study (*131*) seems surprising because the site is relatively inaccessible to solvent; several $^2H_2O-^1H_2O$ exchange studies have reported that ^2H_2O exchanges into the environment of $Y_D^\bullet$ very slowly, with half-decay times of 8 h or longer (*3*, *19*, *48*, *107*, *132*, *133*). By contrast, ^2H_2O exchanges into the environment of $Y_Z^\bullet$ in less than 2 min (*32*; B. A. Diner, personal communication). Also, neutral, lipophilic reductants that reduce $Y_Z^\bullet$ rapidly in Mn-depleted preparations [$k = 10^5-10^7$ M^{-1} s^{-1} (*101*, *102*, *134*, *135*)] reduce $Y_D^\bullet$ very slowly (*134*−*136*) [$k = 6.5 \times 10^2$ M^{-1} s^{-1} for one such compound (*134*)]. Finally, the His to Leu mutation employed in the recent study (*131*) would not be expected to create a cavity near Y_D. Further study of the influence of D2-His189 on Y_D function, especially with mutants designed to create a cavity near Y_D (e.g., H189A or H190S), would seem worthwhile.

In summary, we have measured the kinetics of P_{680}^+ reduction, Y_Z oxidation, Q_A^- oxidation, and $Y_Z^\bullet$ reduction in PSII particles isolated from seven D1-His190 mutants in the presence and absence of imidazole and other small organic bases. On the basis of these measurements, we conclude that D1-His190 is the immediate proton acceptor for Y_Z and that the hydroxyl proton of Y_Z remains bound to D1-His190 throughout the lifetime of $Y_Z^\bullet$, facilitating the reduction of $Y_Z^\bullet$. Because imidazole accelerates both Y_Z oxidation and $Y_Z^\bullet$ reduction in Mn-depleted wild-type* PSII particles, we further conclude that the interaction between Y_Z and D1-His190 is not optimal in Mn-depleted PSII preparations, consistent with previous studies.

ACKNOWLEDGMENT

We are grateful to G. T. Babcock for his enthusiastic interest and helpful advice throughout the course of this project, to B. A. Diner for helpful discussions, for advice concerning the isolation of PSII particles from *Synechocystis* sp. PCC 6803, and for sharing details of his laboratory's unpublished data on D1-His190 mutants, and to G. W. Brudvig, R. D. Britt, M. F. Dunn, W. Junge, F. Rappaport, and M. Hundelt for helpful discussions. In addition, we thank K. Kline and D. P. Pham for help in isolating PSII particles during the initial stages of this project, A. P. Nguyen for maintaining the necessary cultures of *Synechocystis* 6803, and B. A. Diner, G. T. Babcock, K. A. Campbell, and the reviewers for helpful comments on the manuscript.

REFERENCES

1. Debus, R. J. (1992) *Biochim. Biophys. Acta 1102*, 269−352.
2. Britt, R. D. (1996) in *Oxygenic Photosynthesis: The Light Reactions* (Ort, D. R., and Yocum, C. F., Eds.) pp 137−164, Kluwer Academic Publishers, Dordrecht, The Netherlands.
3. Diner, B. A., and Babcock, G. T. (1996) in *Oxygenic Photosynthesis: The Light Reactions* (Ort, D. R., and Yocum, C. F., Eds.) pp 213−247, Kluwer Academic Publishers, Dordrecht, The Netherlands.
4. Bricker, T. M., and Ghanotakis, D. F. (1996) in *Oxygenic Photosynthesis: The Light Reactions* (Ort, D. R., and Yocum, C. F., Eds.) pp 113−136, Kluwer Academic Publishers, Dordrecht, The Netherlands.
5. Yachandra, V. K., Sauer, K., and Klein, M. P. (1996) *Chem. Rev. 96*, 2927−2950.
6. Witt, H. T. (1996) *Ber. Bunsen-Ges. Phys. Chem. 100*, 1923−1942.
7. Renger, G. (1997) *Physiol. Plant. 100*, 828−841.
8. Koulougliotis, D., Tang, X.-S., Diner, B. A., and Brudvig, G. W. (1995) *Biochemistry 34*, 2850−2856.
9. Gilchrist, M. L., Jr., Ball, J. A., Randall, D. W., and Britt, R. D. (1995) *Proc. Natl. Acad. Sci. U.S.A. 92*, 9545−9549.
10. Tang, X.-S., Randall, D. W., Force, D. A., Diner, B. A., and Britt, R. D. (1996) *J. Am. Chem. Soc. 118*, 7638−7639.
11. Force, D. A., Randall, D. W., and Britt, R. D. (1997) *Biochemistry 36*, 12062−12070.
12. Tommos, C., Tang, X.-S., Warncke, K., Hoganson, C. W., Styring, S., McCracken, J., Diner, B. A., and Babcock, G. T. (1995) *J. Am. Chem. Soc. 117*, 10325−10335.

13. Hoganson, C. W., Lydakis-Simantiris, N., Tang, X.-S., Tommos, C., Warncke, K., Babcock, G. T., Diner, B. A., McCracken, J., and Styring, S. (1995) *Photosynth. Res. 46*, 177−184.
14. Babcock, G. T. (1995) in *Photosynthesis: From Light to Biosphere* (Mathis, P., Ed.) Vol. II, pp 209−215, Kluwer Academic Publishers, Dordrecht, The Netherlands.
15. Babcock, G. T., Espe, M., Hoganson, C., Lydakis-Simantiris, N., McCracken, J., Shi, W., Styring, S., Tommos, C., and Warncke, K. (1997) *Acta Chem. Scand. 51*, 533−540.
16. Hoganson, C. W., and Babcock, G. T. (1997) *Science 277*, 1953−1956.
17. Blomberg, M. R., Siegbahn, P. E., Styring, S., Babcock, G. T., Åkermark, B., and Korall, P. (1997) *J. Am. Chem. Soc. 119*, 8285−8292.
18. Tommos, C., and Babcock, G. T. (1998) *Acc. Chem. Res. 31*, 18−25.
19. Tommos, C., McCracken, J., Styring, S., and Babcock, G. T. (1998) *J. Am. Chem. Soc.* (in press).
20. Tommos, C., Hoganson, C. W., Di Valentin, M., Lydakis-Simantiris, N., Dorlet, P., Westphal, K., Chu, H.-A., McCracken, J., and Babcock, G. T. (1998) *Curr. Opin. Chem. Biol. 2*, 244−252.
21. Szalai, V. A., Kühne, H., Lakshmi, K. V., Eaton, G. R., Eaton, S. S., and Brudvig, G. W. (1998) *Biophys. J. 74*, A75.
22. Dorlet, P., Di Valentin, M., Babcock, G. T., and McCracken, J. L. (1998) *J. Phys. Chem.* (in press).
23. Peloquin, J. M., Campbell, K. A., and Britt, R. D. (1998) *J. Am. Chem. Soc.* (in press).
24. Force, D. A., Randall, D. W., Britt, R. D., Tang, X.-S., and Diner, B. A. (1995) *J. Am. Chem. Soc. 117*, 12643−12644.
25. Diner, B. A., Tang, X.-S., Zheng, M., Dismukes, G. C., Force, D. A., Randall, D. W., and Britt, R. D. (1995) in *Photosynthesis: From Light to Biosphere* (Mathis, P., Ed.) Vol. II, pp 229−234, Kluwer Academic Publishers, Dordrecht, The Netherlands.
26. Tang, X.-S., Zheng, M., Chisholm, D. A., Dismukes, G. C., and Diner, B. A. (1996) *Biochemistry 35*, 1475−1484.
27. Un, S., Tang, X.-S., and Diner, B. A. (1996) *Biochemistry 35*, 679−684.
28. Campbell, K. A., Peloquin, J. M., Diner, B. A., Tang, X.-S., Chisholm, D. A., and Britt, R. D. (1997) *J. Am. Chem. Soc. 119*, 4787−4788.
29. Noguchi, T., Inoue, Y., and Tang, X.-S. (1997) *Biochemistry 36*, 14705−14711.
30. Haumann, M., and Junge, W. (1996) in *Oxygenic Photosynthesis: The Light Reactions* (Ort, D. R., and Yocum, C. F., Eds.) pp 165−192, Kluwer Academic Publishers, Dordrecht, The Netherlands.
31. Haumann, M., Bögershausen, O., Cherepanov, D., Ahlbrink, R., and Junge, W. (1997) *Photosynth. Res. 51*, 193−208.
32. Ahlbrink, R., Haumann, M., Cherepanov, D., Bögershausen, O., Mulkidjanian, A., and Junge, W. (1998) *Biochemistry 37*, 1131−1142.
33. Eckert, H.-J., and Renger, G. (1988) *FEBS Lett. 236*, 425−431.
34. Babcock, G. T., Barry, B. A., Debus, R. J., Hoganson, C. W., Atamian, M., McIntosh, L., Sithole, I., and Yocum, C. F. (1989) *Biochemistry 28*, 9557−9565.
35. Haumann, M., and Junge, W. (1994) *Biochemistry 33*, 864−872.
36. Haumann, M., Bögershausen, O., and Junge, W. (1994) *FEBS Lett. 355*, 101−105.
37. Bögershausen, O., and Junge, W. (1995) *Biochim. Biophys. Acta 1230*, 177−185; *Biochim. Biophys. Acta 1232*, 89.
38. Kretschmann, H., Schlodder, E., and Witt, H. T. (1996) *Biochim. Biophys. Acta 1274*, 1−8.
39. Haumann, M., Drevenstedt, W., Hundelt, M., and Junge, W. (1996) *Biochim. Biophys. Acta 1273*, 237−250.
40. Hundelt, M., Haumann, M., and Junge, W. (1997) *Biochim. Biophys. Acta 1321*, 47−60.
41. Rappaport, F., and Lavergne, J. (1997) *Biochemistry 36*, 15294−15302.
42. Rappaport, F., Blanchard-Desce, M., and Lavergne, J. (1994) *Biochim. Biophys. Acta 1184*, 178−192.
43. Mulkidjanian, A., Cherepanov, D., Haumann, M., and Junge, W. (1996) *Biochemistry 35*, 3093−3107.
44. Svensson, B., Etchebest, C., Tuffery, P., Van Kan, P., Smith, J., and Styring, S. (1996) *Biochemistry 35*, 14486−14502.
45. Svensson, B., Vass, I., Cedergren, E., and Styring, S. (1990) *EMBO J. 9*, 2051−2059.
46. Ruffle, S. V., Donnelly, D., Blundell, T. L., and Nugent, J. H. A. (1992) *Photosynth. Res. 34*, 287−300.
47. Tommos, C., Davidsson, L., Svensson, B., Madsen, C., Vermaas, W. F. J., and Styring, S. (1993) *Biochemistry 32*, 5436−5441.
48. Tang, X.-S., Chisholm, D. A., Dismukes, G. C., Brudvig, G. W., and Diner, B. A. (1993) *Biochemistry 32*, 13742−13748.
49. Hienerwadel, R., Boussac, A., Breton, J., Diner, B. A., and Berthomieu, C. (1997) *Biochemistry 36*, 14712−14723.
50. Diner, B. A., Nixon, P. J., and Farchaus, J. W. (1991) *Curr. Opin. Struct. Biol. 1*, 546−554.
51. Nixon, P. J., and Diner, B. A. (1994) *Biochem. Soc. Trans. 22*, 338−343.
52. Roffey, R. A., Kramer, D. M., Govindjee, and Sayre, R. T. (1994) *Biochim. Biophys. Acta 1185*, 257−270.
53. Roffey, R. A., van Wijk, K. J., Sayre, R. T., and Styring, S. (1994) *J. Biol. Chem. 269*, 5115−5121.
54. Chu, H.-A., Nguyen, A. P., and Debus, R. J. (1995) *Biochemistry 34*, 5839−5858.
55. Chu, H.-A., Nguyen, A. P., and Debus, R. J. (1994) *Biochemistry 33*, 6137−6149.
56. Toney, M. D., and Kirsch, J. F. (1989) *Science 243*, 1485−1488.
57. Smith, H. B., and Hartman, F. C. (1991) *Biochemistry 30*, 5172−5177.
58. Zhukovsky, E. A., Robinson, P. R., and Oprian, D. D. (1991) *Science 251*, 558−560.
59. Toney, M. D., and Kirsch, J. F. (1992) *Protein Sci. 1*, 107−119.
60. Phillips, M. A., Hedstrom, L., and Rutter, W. J. (1992) *Protein Sci. 1*, 517−521.
61. Brooks, B., and Benisek, W. F. (1992) *Biochem. Biophys. Res. Commun. 184*, 1386−1392.
62. Sekimoto, T., Matsuyama, T., Fukui, T., and Tanizawa, K. (1993) *J. Biol. Chem. 268*, 27039−27045.
63. Perona, J. J., Hedstrom, L., Wagner, R. L., Rutter, W. J., Craik, C. S., and Fletterick, R. J. (1994) *Biochemistry 33*, 3252−3259.
64. Dhalla, A. M., Li, B., Alibhai, M. F., Yost, K. J., Hemminsen, J. M., Atkins, W. M., Schineller, J., and Villafrance, J. J. (1994) *Protein Sci. 3*, 476−481.
65. Harpel, M. R., and Hartman, F. C. (1994) *Biochemistry 33*, 5553−5561.
66. Tu, C., Silverman, D. N., Forsman, C., Jonsson, B.-H., and Lindskog, S. (1989) *Biochemistry 28*, 7913−7918.
67. Carter, P., Abrahmsén, L., and Wells, J. A. (1991) *Biochemistry 30*, 6142−6148.
68. den Blaauwen, T., and Canters, G. W. (1993) *J. Am. Chem. Soc. 115*, 1121−1129.
69. den Blaauwen, T., Hoitink, C. W. G., Canters, G. W., Han, J., Loehr, T. M., and Sanders-Loehr, J. (1993) *Biochemistry 32*, 12455−12464.
70. Barrick, D. (1994) *Biochemistry 33*, 6546−6554.
71. DePillis, G. D., Decatur, S. M., Barrick, D., and Boxer, S. G. (1994) *J. Am. Chem. Soc. 116*, 6981−6982.
72. McRee, D. E., Jensen, G. M., Fitzgerald, M. M., Siegel, H. A., and Goodin, D. B. (1994) *Proc. Natl. Acad. Sci. U.S.A. 91*, 12847−12851.
73. Chu, H.-A., Nguyen, A. P., and Debus, R. J. (1995) in *Photosynthesis: From Light to Biosphere* (Mathis, P., Ed.) Vol. II, pp 439−442, Kluwer Academic Publishers, Dordrecht, The Netherlands.
74. Rippka, R., Deruelles, J., Waterbury, J. B., Herdman, M., and Stanier, R. Y. (1979) *J. Gen. Microbiol. 111*, 1−61.
75. Vermaas, W. F. J. (1994) *Biochim. Biophys. Acta 1187*, 181−186.

76. Tang, X.-S., and Diner, B. A. (1994) *Biochemistry 33*, 4594−4603.
77. Bernard, M. T., MacDonald, G. M., Nguyen, A. P., Debus, R. J., and Barry, B. A. (1995) *J. Biol. Chem. 270*, 1589−1594.
78. Peiffer, W. E., Ingle, R. T., and Ferguson-Miller, S. (1990) *Biochemistry 29*, 8696−8701.
79. Lichtenthaler, H. K. (1987) *Methods Enzymol. 148*, 350−382.
80. Wingo, W. J., and Emerson, G. M. (1975) *Anal. Chem. 47*, 351−352.
81. MacDonald, G. M., Boerner, R. J., Everly, R. M., Cramer, W. A., Debus, R. J., and Barry, B. A. (1994) *Biochemistry 33*, 4393−4400.
82. van Gorkom, H. J. (1974) *Biochim. Biophys. Acta 347*, 439−442.
83. Vassiliev, I. R., Jung, Y. S., Mamedov, M. D., Semenov, A. Y., and Golbeck, J. H. (1997) *Biophys. J. 72*, 301−315.
84. Buser, C. A., Thompson, L. K., Diner, B. A., and Brudvig, G. W. (1990) *Biochemistry 29*, 8977−8985.
85. Buser, C. A. (1993) Electron-Transfer Reactions in Photosystem II, Ph.D. Dissertation, Yale University, New Haven, CT.
86. Pulles, M. P. J., van Gorkom, H. J., and Verschoor, G. A. M. (1976) *Biochim. Biophys. Acta 440*, 98−106.
87. Gerken, S., Dekker, J. P., Schlodder, E., and Witt, H. T. (1989) *Biochim. Biophys. Acta 977*, 52−61.
88. Metz, J. G., Nixon, P. J., Rögner, M., Brudvig, G. W., and Diner, B. A. (1989) *Biochemistry 28*, 6960−6969.
89. Mathis, P., and Vermeglio, A. (1975) *Biochim. Biophys. Acta 369*, 371−381.
90. Mathis, P., and Sétif, P. (1981) *Isr. J. Chem. 21*, 316−320.
91. Dekker, J. P., van Gorkom, H. J., Brok, M., and Ouwehand, L. (1984) *Biochim. Biophys. Acta 764*, 301−309.
92. Schatz, G. H., and van Gorkom, H. J. (1985) *Biochim. Biophys. Acta 810*, 283−294.
93. Diner, B. A., and de Vitry, C. (1984) in *Advances in Photosynthesis Research* (Sybesma, C., Ed.) Vol. I, pp 407−411, Martinus Nijhoff, The Hague, The Netherlands.
94. Gerken, S., Brettel, K., Schlodder, E., and Witt, H. T. (1988) *FEBS Lett. 237*, 69−75.
95. van Best, J. A., and Mathis, P. (1978) *Biochim. Biophys. Acta 503*, 178−188.
96. Conjeaud, H., Mathis, P., and Paillotin, G. (1979) *Biochim. Biophys. Acta 546*, 280−291.
97. Conjeaud, H., and Mathis, P. (1980) *Biochim. Biophys. Acta 590*, 353−359.
98. Reinman, S., Mathis, P., Conjeaud, H., and Stewart, A. (1981) *Biochim. Biophys. Acta 635*, 429−433.
99. Conjeaud, H., and Mathis, P. (1986) *Biophys. J. 49*, 1215−1221.
100. Christen, G., Karge, M., Eckert, H.-J., and Renger, G. (1997) *Photosynthetica 33*, 529−539.
101. Babcock, G. T., and Sauer, K. (1975) *Biochim. Biophys. Acta 396*, 48−62.
102. Yerkes, C. T., and Babcock, G. T. (1980) *Biochim. Biophys. Acta 590*, 360−372.
103. Hoganson, C. W., Ghanotakis, D. F., Babcock, G. T., and Yocum, C. F. (1989) *Photosynth. Res. 22*, 285−293.
104. Diner, B. A., and Nixon, P. J. (1992) *Biochim. Biophys. Acta 1101*, 134−138.
105. Danielsen, E., Bauer, R., Hemmingsen, L., Bjerrum, M. J., Butz, T., Tröger, W., Canters, G. W., den Blaauwen, T., and Van Pouderoyen, G. (1995) *Eur. J. Biochem. 233*, 554−560.
106. Newmyer, S. L., Sun, J., Loehr, T. M., and Ortiz de Montellano, P. R. (1996) *Biochemistry 35*, 12788−12795.
107. Mino, H., Astashkin, A. V., and Kawamori, A. (1997) *Spectrochim. Acta, Part A 53*, 1465−1483.
108. Berthomieu, C., Hienerwadel, R., Boussac, A., Breton, J., and Diner, B. A. (1998) *Biochemistry* (in press).
109. Hoganson, C. W., Sahlin, M., Sjöberg, B.-M., and Babcock, G. T. (1996) *J. Am. Chem. Soc. 118*, 4672−4679.
110. Dole, F., Diner, B. A., Hoganson, C. W., Babcock, G. T., and Britt, R. D. (1997) *J. Am. Chem. Soc. 119*, 11540−11541.
111. Berthomieu, C., Nabedryk, E., Mäntele, W., and Breton, J. (1990) *FEBS Lett. 269*, 363−367.
112. Noguchi, T., Ono, T.-A., and Inoue, Y. (1992) *Biochemistry 31*, 5953−5956.
113. Berthomieu, C., Nabedryk, E., Breton, J., and Boussac, A. (1992) in *Research in Photosynthesis* (Murata, N., Ed.) Vol. II, pp 53−56, Kluwer Academic Publishers, Dordrecht, The Netherlands.
114. Hienerwadel, R., Boussac, A., Breton, J., and Berthomieu, C. (1996) *Biochemistry 35*, 15447−15460.
115. Zhang, H. M., Razeghifard, M. R., Fischer, G., and Wydrzynski, T. (1997) *Biochemistry 36*, 11762−11768.
116. Berthomieu, C., Boussac, A., Mäntele, W., Breton, J., and Nabedryk, E. (1992) *Biochemistry 31*, 11460−11471.
117. Araga, C., Akabori, K., Sasaki, J., Maeda, A., Shiina, T., and Toyoshima, Y. (1993) *Biochim. Biophys. Acta 1142*, 36−42.
118. Noguchi, T., Ono, T.-A., and Inoue, Y. (1993) *Biochim. Biophys. Acta 1143*, 333−336.
119. Fersht, A. R. (1985) *Enzyme Mechanism and Structure*, 2nd ed., W. H. Freeman and Company, New York.
120. Garrett, T. P. J., Clingeleffer, D. J., Guss, J. M., Rogers, S. J., and Freeman, H. C. (1984) *J. Biol. Chem. 259*, 2822−2825.
121. Nar, H., Messerschmidt, A., Huber, M., van de Camp, M., and Canters, G. W. (1992) *FEBS Lett. 306*, 119−124.
122. Marks, R. H. L., and Miller, R. D. (1979) *Arch. Biochem. Biophys. 195*, 103−111.
123. Tang, X.-S., Diner, B. A., Britt, R. D., and Babcock, G. T. (1996) *Photochem. Photobiol. 63*, 81s.
124. Schilstra, M. J., Rappaport, F., Nugent, J. H. A., Barnett, C. J., and Klug, D. R. (1998) *Biochemistry 37*, 3974−3981.
125. Karge, M., Irrgang, K.-D., Sellin, S., Feinäugle, R., Liu, B., Eckert, H.-J., Eichler, H. J., and Renger, G. (1996) *FEBS Lett. 378*, 140−144.
126. Reinman, S., and Mathis, P. (1981) *Biochim. Biophys. Acta 635*, 249−258.
127. Yerkes, C. T., Babcock, G. T., and Crofts, A. R. (1983) *FEBS Lett. 158*, 359−363.
128. Moser, C. C., Keske, J. M., Warncke, K., Farid, R. S., and Dutton, P. L. (1992) *Nature 355*, 796−802.
129. Gray, H. B., and Winkler, J. R. (1996) *Annu. Rev. Biochem. 65*, 537−561.
130. Moser, C. C., and Dutton, P. L. (1996) in *Protein Electron Transfer* (Bendall, D. S., Ed.) pp 1−21, BIOS Scientific Publishers, Oxford, U.K.
131. Kim, S., Liang, J., and Barry, B. A. (1997) *Proc. Natl. Acad. Sci. U.S.A. 94*, 14406−14411.
132. Rodriguez, I. D., Chandrashekar, T. K., and Babcock, G. T. (1987) in *Progress in Photosynthesis Research* (Biggins, J., Ed.) Vol. I, pp 471−474, Martinus Nijhoff Publishers, Dordrecht, The Netherlands.
133. Evelo, R. G., Hoff, A. J., Dikanov, S. A., and Tyryshkin, A. M. (1989) *Chem. Phys. Lett. 161*, 479−484.
134. Ghanotakis, D. F., Yerkes, C. T., and Babcock, G. T. (1982) *Biochim. Biophys. Acta 682*, 21−31.
135. Babcock, G. T., Ghanotakis, D. F., Ke, B., and Diner, B. A. (1983) *Biochim. Biophys. Acta 723*, 276−286.
136. Lozier, R. H., and Butler, W. L. (1973) *Photochem. Photobiol. 17*, 133−137.
137. Kim, S., and Barry, B. A. (1998) *Biophys. J. 74*, 2588−2600.
138. Kim, S., Ayala, I., Steenhuis, J. J., Gonzalez, E. T., and Barry, B. A. (1998) *Biochim. Biophys. Acta 1364*, 337−360.

BI980510U